DOI: 10.1002/anie.200701920

Organic Electronics

Organic Semiconductors for Solution-Processable Field-Effect Transistors (OFETs)

*Sybille Allard, Michael Forster, Benjamin Souharce, Heiko Thiem, and Ullrich Scherf**

Keywords:
charge-carrier mobility · molecular electronics · organic field-effect transistors · polymers · semiconductors

Dedicated to Professor Klaus Müllen on the occasion of his 60th birthday.

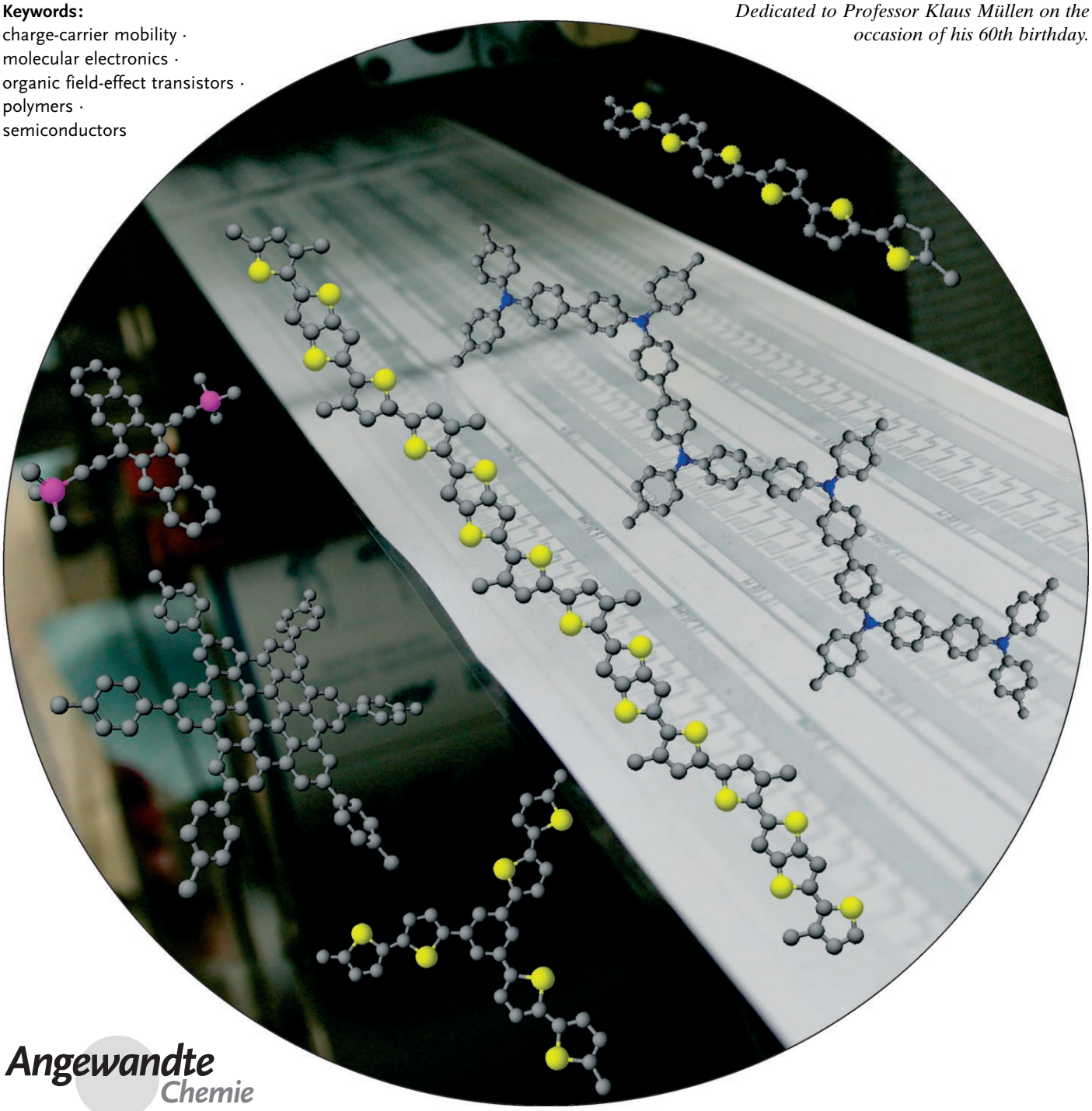

The cost-effective production of flexible electronic components will profit considerably from the development of solution-processable, organic semiconductor materials. Particular attention is focused on soluble semiconductors for organic field-effect transistors (OFETs). The hitherto differentiation between "small molecules" and polymeric materials no longer plays a role, rather more the ability to process materials from solution to homogeneous semiconducting films with optimal electronic properties (high charge-carrier mobility, low threshold voltage, high on/off ratio) is pivotal. Key classes of materials for this purpose are soluble oligoacenes, soluble oligo- and polythiophenes and their respective copolymers, and oligo- and polytriarylamines. In this context, micro- or nanocrystalline materials have the general advantage of somewhat higher charge-carrier mobilities, which, however, could be offset in the case of amorphous, glassy materials by simpler and more reproducible processing.

From the Contents

1. Introduction

Following decades of intensive research, organic field-effect transistors (OFETs) have now laid claim to sustained interest in university and industrial research.[1] What makes the involvement with them so attractive? While the first OFETs adapted directly the construction of classical inorganic field-effect transistors—that is, only the semiconductor consisted of an organic material—in 1998 a group at the Philips Research Laboratories in Eindhoven succeeded in producing an integrated circuit that consisted entirely of organic materials.[1c] This success has opened up completely new areas for application for organic field-effect transistors, particularly for developing cheap electronic components. The first OFETs based solely on organic materials had field-effect charge-carrier mobilities μ_{FET} of less than $10^{-2}\,cm^2V^{-1}s^{-1}$ and were still vastly inferior to the inorganic field-effect transistors based on amorphous silicon (a-Si) as semiconductor ($\mu_{FET}=10^{-1}$–$1\,cm^2V^{-1}s^{-1}$). After 10 years of intensive research solution-processed OFET components are now approaching the field mobilities of amorphous silicon (maximum mobilities μ_{FET} of $0.6\,cm^2V^{-1}s^{-1}$).[2] "Wet chemistry" processing of materials from solution has played a special role in this development, as will be presented in detail herein.

Whereas processing temperatures above 350 °C are required for the application of a-Si layers in the production of inorganic field-effect transistors, organic semiconductors can be applied and processed at significantly lower temperatures. As polymer films, such as polyethylene terephthalate (PET), that retain their shape only up to about 180 °C are to be used as substrate for cost-effective and flexible circuits in organic electronics, the application of inorganic semiconductors such as a-Si is not feasible. Thus, novel applications are possible in organic electronics for which flexible circuits are imperative, for example, electronic paper.

In OFETs, the individual components (electrodes, semiconductors, insulators, possibly encapsulation) can be applied by different techniques: On the one hand, the layers can be deposited from the gas phase in analogy to the processing of most inorganic semiconductors (physical vapor deposition (PVD), chemical vapor deposition (CVD), sputtering), whereas on the other hand inexpensive solution techniques (e.g., spin coating, inkjet printing, and screen printing) are possible. Their use depends on the physical characteristics of the components, such as vapor pressure, stability, and solubility. From the outset the nature of the materials frequently sets the boundaries for their processing (for example, with metals as electrode material; with (almost) insoluble organic semiconductors, such as pentacene or phthalocyanines, which are only processable through gas-phase processes; or with polymeric semiconductors, which owing to their extremely low vapor pressure cannot be processed in the gas phase). The use of materials that can be applied from solution should allow large-area processing in roll-to-roll methods, for example, for the electronic control of large active-matrix displays or in electronic labels. Moreover, it is expected that the avoidance of slow and cost-intensive vapor deposition methods in high vacuum will bring cost advantages. For use in electronic labels, so-called RFID tags (radio frequency identification tags), a production cost of less than one cent per label will be required.[3]

For many complex chemical, physical, and technological questions that involve all OFET components (conductors, semiconductors, and insulators) and their interplay, the organic semiconductor used is as always a key component. An extremely high level of purity and reliability of the material, for example, is demanded for large-scale applications. In this review, we would therefore like to present

[*] Dr. S. Allard, Dr. M. Forster, B. Souharce, Prof. Dr. U. Scherf
FB C—Makromolekulare Chemie und
Institut für Polymertechnologie
Bergische Universität Wuppertal
Gaussstrasse 20, 42119 Wuppertal (Germany)
Fax: (+49) 202-439-3880
E-mail: scherf@uni-wuppertal.de
Homepage: http://www.chemie.uni-wuppertal.de/poly/
Dr. H. Thiem
Evonik Degussa
Creavis Technologies & Innovation
Paul-Baumann-Strasse 1, 45772 Marl (Germany)

innovative approaches to the synthesis of organic semiconducting compounds that can be processed from solution and highlight their potential as semiconductors in OFETs. Both low molecular weight compounds ("small molecules" and oligomers) and polymeric semiconductors are suitable for this purpose. As there are still very few research results in the area of soluble n-semiconductors, we will generally restrict ourselves to the discussion of p-semiconductors. Initially, in Section 2, alternatives for the construction of OFETs and their most important characteristics will be discussed briefly, and differences and commonalities in the use of low molecular weight and polymeric semiconductors will be highlighted. In Section 3, the synthesis and properties of low molecular weight and polymeric semiconductors will be discussed in more detail.

2. Organic Field-effect transistors: Construction and Functionality

Field-effect transistors based on organic materials are constructed primarily according to the principle of the thin film transistor (TFT). They can be constructed in two different configurations: the top-gate and the bottom-gate configuration (Figure 1).[4] In the top-gate configuration, the two electrodes (source and drain) between which the current flow is to be actuated are situated on a substrate. On top of this substrate is located an organic semiconductor layer, which in turn is separated from the control electrode (the gate electrode) by a dielectric layer. In this way, the so-called power channel is established as the region that is enclosed by the three electrodes. The channel length is determined by the distance between the source and drain electrodes; the channel width comes from the length of the source and drain electrodes and is maximized through the use of comb structures.

Sybille Allard studied chemistry at the Johannes-Gutenberg Universität Mainz where she gained her PhD in 2003 in the group of Prof. Dr. R. Zentel on the synthesis and structuring of oligothiophenes. Since then she has untertaken postdoctoral studies on various projects at the Bergische Universität Wuppertal.

Michael Forster studied chemistry at the TU München and gained his PhD in 2000 with Prof. Dr. K. Müllen at the MPI für Polymerforschung/Universität Mainz (new conjugated polyarylenes with ladder-type structure). He spent the next 2 years on postdoctoral studies at the Universität Potsdam and in 2002 he moved with Prof. U. Scherf to the Bergische Universität Wuppertal. There, as project leader, he coordinates the research on conjugated polymers and is at the same time head of department for synthesis and development at the Institut für Polymertechnologie.

Heiko Thiem studied chemistry at the Universität Bayreuth. He completed doctoral work in 2005 under the supervision of Prof. P. Strohriegl in the area of semiconductor polymers and oligomers for use in optoelectronic devices in close cooperation with Merck KGaA (Southampton) and Philips (Eindhoven). Since January 2006 he has been with Evonik Industries in the Science to Business Center Nanotronics, where he is responsible for the development of new solution-processable semiconductors and other components for OFETs.

Benjamin Souharce completed his studies in materials science at the Université Paul Sabatier in Toulouse and at the Université de Rouen in 2003. He completed his Diplomarbeit at the Gerhard-Mercator-Universität Duisburg on liquid-crystal polymers. Since 2004 he has been working towards a PhD under the leadership of Prof. U. Scherf at the Bergische Universität Wuppertal in the area of triphenylamine-containing semiconductor polymer materials for use in OFETs in close cooperation with the S2B-Center Nanotronics (Marl) of Evonik Industries.

Ullrich Scherf studied chemistry at the Friedrich-Schiller-Universität in Jena and gained his PhD in 1988 under Prof. H.-H. Hörhold on the synthesis of organic semiconductors of the PPV type and carbonization of polymer films. He then spent a year at the Institut für Tierphysiologie, Sächsische Akademie der Wissenschaften zu Leipzig, in the group of Prof. H. Penzlin. In 1990 he moved to the Max-Planck-Institut für Polymerforschung where he gained his habilitation under Prof. K. Müllen in 1996 on polyarylene-type ladder polymers. From 2000 to 2002 he was professor for polymer chemistry at the Universität Potsdam, and since 2002 has been professor for macromolecular chemistry at the Bergische Universität Wuppertal.

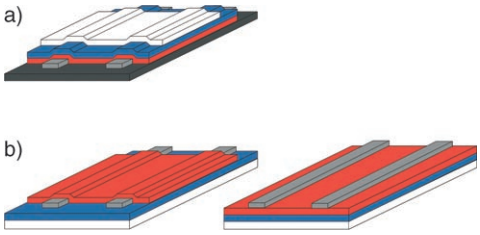

Figure 1. Construction of a field-effect transistor: a) top-gate configuration; b) bottom-gate configuration, left: bottom contact, right: top contact; black: substrate; gray: source and drain electrodes; red: semiconductor; blue: isolator; white: gate electrodes.

In the top-gate construction, the semiconductor layer is applied to a suitable substrate, for example, a polymer film, on which are also located the source and drain electrodes, followed by an insulator layer. The finish in this case is a top-gate electrode. In the bottom-gate configuration, the gate electrode is situated directly on the substrate; often a silicon wafer functions as both substrate and gate. The dielectric, often thermallly grown silicon dioxide, is situated on top. In a bottom-contact construction, the source and drain electrodes are above, followed by the semiconductor layer. In the top-contact configuration, the semiconductor layer is situated directly above the insulator, and the source and drain electrodes are attached right on top. However, the top-contact configuration is often difficult to realize with organic FETs. Attachment of the electrodes is usually carried out thermally with metals and can destroy thin organic layers; moreover, metal atoms can diffuse into the organic material. The top-gate configuration is favored for printed transistors, for which the individual components are applied sequentially. Conducting polymers such as (doped) polyaniline or polyethylenedioxythiophene/poly(styrene sulfonic acid) (PEDOT/PSS) serve as electrodes in OFETs totally constructed of organic materials, and insulating polymers with high capacity, such as polyvinylphenol (PVP), poly(vinyl alcohol) (PVA), polyimide (PI), or poly(methyl methacrylate) (PMMA) are used as dielectric layer.

The basic circuit of a bottom-gate OFET is shown in Figure 2. The source electrode is earthed, and all other voltages are given in relation to this electrode. If a negative voltage U_G is applied to the gate electrode (with p-semiconductors), an electric field is induced perpendicular to the layers. Enrichment in positive charge carriers occurs at the interface between semiconductor and gate insulator as a consequence. If at the same time a voltage U_D is applied at the drain electrode, holes can be transported from the source electrode to the drain electrode. This conducting state is called the "on" state; $U_G = 0$ defines the "off" state.

The most important characteristics of a field-effect transistor are the threshold voltage U_t, the on/off ratio I_{on}/I_{off}, and the charge-carrier mobility μ_{FET}. The threshold voltage U_t characterizes the voltage U_D at which the field effect sets in; it is primarily a measure of the number of the charge-carrier traps in the semiconductor interface that must be overcome. In organic semiconductors, there are localized trap states of variable depth which after application of a voltage first have to be filled with charge carries before a current can flow between source and drain electrodes. A greatest possible difference between the two states I_{on} and I_{off} is in turn fundamental for a clear difference between the states "0" and "1" in electronic circuits (e.g., inverter circuits). The on/off ratio is defined as the ratio of the source–drain current in the "on" and the "off" state of the field-effect transistor. The charge-carrier mobility μ_{FET} in turn primarily determines the size of the voltage to be applied and thus the power consumption of the transistor (other influencing factors are, for example, the dimensions of the components).

The output characteristic curve of the transistor (i.e., a plot of the source–drain current I_D against the drain voltage U_D at different gate voltages U_G) is used to determine the charge-carrier mobility. An output characteristic curve for poly(3-hexylthiophene) (P3HT) as semiconductor is shown in Figure 3.[5] Two regions of the characteristic curve can be differentiated: at low drain voltage, the source–drain current rises almost linearly (linear region), later to convert into a saturation region. The source–drain current in the linear region can be defined according to Equation (1), in which L is

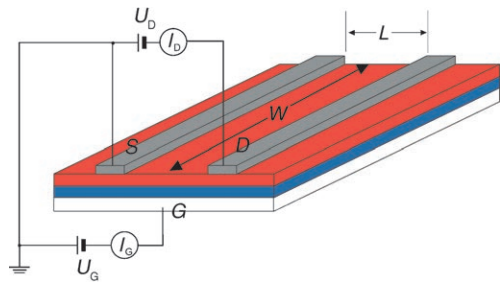

Figure 2. OFET circuit: U_D: drain voltage; I_D: drain current; L: channel length; W: channel width; S: source electrode; D: drain electrode; G: gate electrode; U_G: gate voltage; I_G: gate current.

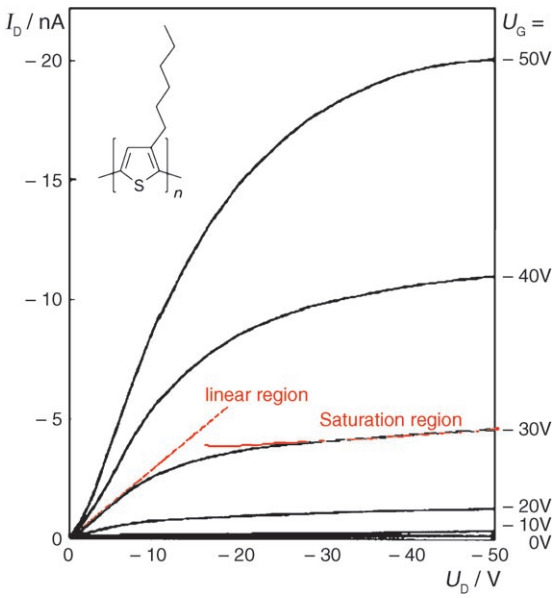

Figure 3. OFET output characteristics plot for a device with poly(3-heyxlthiophene) as semiconductor.

the channel length, W the channel width, C_i the capacitance per unit area of the insulator layer, U_t the threshold voltage, and $\mu_{FET,lin}$ the mobility in the linear region. The field-effect mobility for the linear region can be calculated directly from the slope of the so-called transfer characteristic curve, a plot of the source–drain current against the gate voltage at constant drain voltage. The slope is calculated according to Equation (2), which is based on the assumption $U_D \ll (U_G - U_t)$. In the second region of the output characteristic curve (the saturation region), Equation (3) applies for the source–drain current when $U_D > (U_G - U_t)$. The charge-carrier mobility $\mu_{FET,sat}$ in the saturation region can be calculated from the slope of the current–voltage curve in a plot of $I_D^{1/2}$ against U_G.

$$I_D = \frac{W C_i}{L} \mu_{FET,lin} \left[(U_G - U_t) U_D - \frac{U_D^2}{2} \right] \quad (1)$$

$$\frac{\partial I_D}{\partial U_G} = \frac{W C_i}{L} \mu_{FET,lin} U_D \quad (2)$$

$$I_D = \frac{W C_i \mu_{FET,sat}}{2L} (U_G - U_t)^2 \quad (3)$$

These equations are only valid under the assumption of a constant charge-carrier mobility in the interval under consideration. However, as in the case of organic semiconductors the mobility is usually significantly dependent on the gate voltage and the temperature, Equations (2) and (3) can only be used to estimate the charge-carrier mobility. The model was further refined by Horowitz et al., who developed a mathematical model to determine voltage- and temperature-dependent charge-carrier mobility, but these considerations will not be discussed further herein.[6]

3. Soluble Organic Semiconductors for Use in OFETs

As mentioned previously, "small molecules" or oligomers as well as polymers are suitable organic semiconductors for OFET applications. Owing to their crystallinity, "small" molecules often have the advantage that they order themselves very well in the solid state. This generally leads to a high charge-carrier mobility, as the mobility depends primarily on the intermolecular interactions, but frequently also to a limited processability of the compounds from solution (usually owing to low solubility).

There are various solutions to this dilemma (Figure 4). One possibility is the use of soluble processable precursor compounds of the actual insoluble semiconductor. This method has been employed very successfully, particularly for pentacene and derived acenes. A second possibility is the insertion of solubilizing substituents, for example, terminal alkyl groups. If these groups are inserted into the α- and ω-positions of almost insoluble oligothiophenes, not only is the solubility increased dramatically, but charge-carrier mobility is also improved relative to that of the unsubstituted compounds, because of the higher order of the molecules in the crystal.[7] If, however, oligothiophenes are substituted by

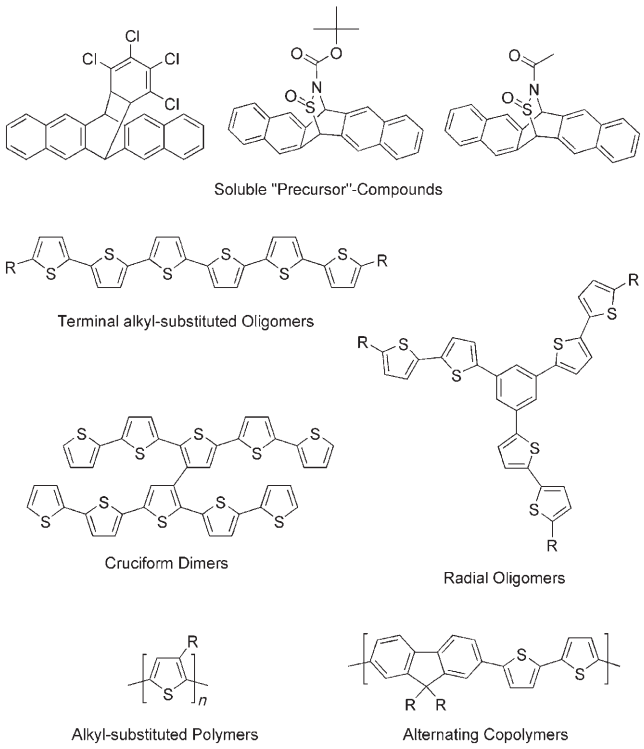

Figure 4. Examples of strategies for solubilizing organic semiconductors.

alkyl groups in 3-position of the thiophene rings forming the chain, the charge-carrier mobility is considerably reduced relative to that of the unsubstituted compounds owing to a distortion of the intra- and intermolecular order arising from the insertion of the side chains. The solubility can also be increased through the synthesis of angulated molecules (e.g., star-shaped or dendritic oligomers, dimers with crosslike structure ("cruciforms"), or branched or hyperbranched polymers).[8] Strategies for the solubilization of linear semiconducting polymers include the attachment of alkyl substituents, preferably in a regioregular manner, or the preparation of alternating copolymers.

A major problem in the use of organic semiconductors is the instability of the materials to light, atmospheric oxygen, and humidity, or a combination of these stress factors, which limits the shelf life of these components. The combination of light and oxygen is regarded as particularly critical. This problem is well documented, for example, for oligo- and polythiophenes.[9] The penetration of air and humidity can be partially prevented by encapsulation of the devices, but alternative semiconducting materials that increase the stability of the devices are also being sought. The key factor is the shelf life, that is, the time for which the components may be stored without a sacrifice in electronic function. The instability (oxidation sensitivity) of the compounds often lies in the low ionization potential, that is, a high-lying HOMO energy level. The HOMO energy is correlated among others with the π electron topology and the effective conjugation length of the compounds. Within a particular class of compounds (e.g. acenes and oligothiophenes) an increased effective conjuga-

tion length leads to energy-rich HOMO levels and thus to an increased susceptibility towards oxidation. The effective conjugation length in oligo- and polythiophenes is determined primarily by the number and the substitution of the conjugated building blocks and the resulting chain conformation. The latter is greatly influenced by the insertion of substituents if these result in a distortion of the planarity of the molecular construction. The compounds are then less readily oxidizable, but the insertion of bulky substituents usually leads to a reduced charge-carrier mobility through lowering of the intermolecular order. In contrast, electron-rich substituents (alkoxy groups) lead to a further increase in the HOMO energy level. Electron-rich polythiophenes, such as poly(3,4-ethylenedioxy-2,5-thiophene) (PEDOT), are only stable in the oxidized ("doped") state (PEDOT/PSS; poly(styrene sulfonic acid) (PSS) as polymeric counterion of the oxidized PEDOT chains) and are used as organic conductors (e.g. for electrodes). In contrast, electron-deficient substituents on oligothiophenes (e.g. 2,2-dicyanovinyl-1) lead to electronic stabilization.[10] In this section many such structure–property relationships are described.

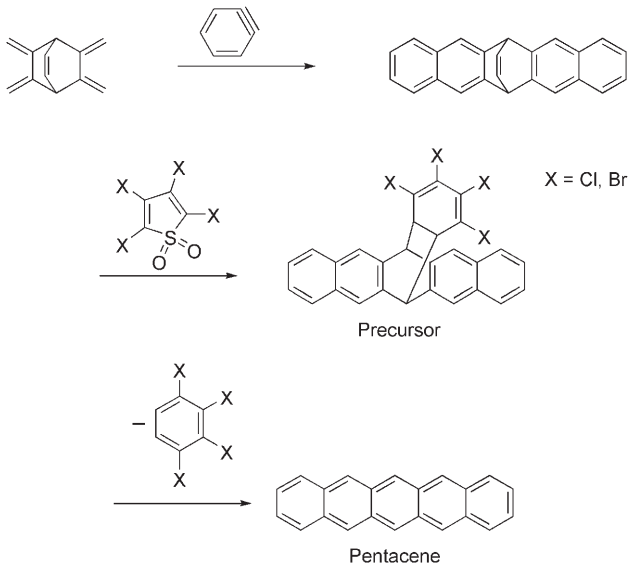

Scheme 1. Synthesis of a 1,2,3,4-tetrahalocyclohexa-1,3-diene-bridged pentacene precursor.

3.1. Low Molecular Weight Compounds

3.1.1. Acenes and Heteroacenes

Whereas among the low molecular weight organic compounds the highest charge-carrier mobilities in a single crystal were measured for rubrene ($20\ cm^2V^{-1}s^{-1}$), pentacene has the highest charge-carrier mobility in polycrystalline film (up to $5\ cm^2V^{-1}s^{-1}$).[11] Moreover, pentacene is characterized by its adequate stability towards oxygen and humidity. However, since it is almost insoluble in the common organic solvents, it is processed solely by vacuum deposition.

Different strategies have been developed for the application of thin pentacene films from solution. One method consists of the synthesis of a soluble precursor, which after film formation is converted into the target material pentacene. The first "pentacene precursor", described by Müllen and co-workers in 1996 (Scheme 1),[12] was a 6,13-dihydropentacene bridged at the 6,13-positions with 1,2,3,4-tetrachloro- or 1,2,3,4-tetrabromocyclohexa-1,3-diene, which was synthesized from a 6,13-vinylene-bridged dihydropentacene that was first prepared in a double Diels–Alder reaction with dehydrobenzene generated in situ. This precursor was then converted into the target compound in a further Diels–Alder reaction with tetrahalothiophene dioxide. The resulting "pentacene precursor" is soluble in common organic solvents. After application of a thin film onto a suitable substrate by spin coating, the bridging group can be eliminated thermally at 200 °C as 1,2,3,4-tetrahalobenzene in a retro-Diels–Alder reaction. The unsubstituted pentacene remains as a polycrystalline film. Charge-carrier mobilities μ of up to $0.2\ cm^2V^{-1}s^{-1}$ have been measured in field-effect transistors with pentacene as semiconductor prepared in this way.

Drawbacks of the pentacene precursor developed by K. Müllen and co-workers are the multistep and thus inconvenient synthetic method and the high temperature that is necessary for elimination of the bridging groups. In 2002 a research group from IBM published a simpler precursor synthesis that started directly from pentacene itself (Scheme 2).[13] Pentacene reacts as diene in a Diels–Alder reaction with an *N*-sulfinylacetamide, and is likewise bridged

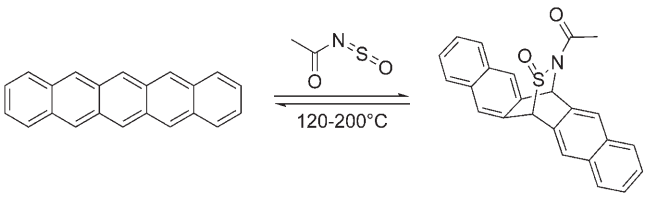

Scheme 2. Synthesis of a pentacene precursor by reaction of pentacene with *N*-sulfinylacetamide.

in the 6,13-positions. The *N*-sulfinylacetamide can be eliminated in a retro-Diels–Alder reaction at 120–200 °C with regeneration of pentacene. Organic field-effect transistors (OEFT) with pentacene films prepared in this way showed a charge-carrier mobility μ of $0.29\ cm^2V^{-1}s^{-1}$ at a drain voltage of $U_D = -20$ V in the linear region of the transfer characteristics plot, and a charge-carrier mobility in the saturated region of $0.89\ cm^2V^{-1}s^{-1}$. The on/off ratio was 2×10^7. Subramanian and co-workers also attempted to apply this pentacene precursor onto the active layer by inkjet printing of suitable solutions and investigated the dependency of the charge-carrier mobility on the temperature and the duration of the final thermal reaction.[14] They used a solution of the pentacene precursor in anisole and applied the semiconductor layer by inkjet printing in a bottom-gate configuration on gold source and drain electrodes and silicon dioxide as gate insulator. It was shown that the degree of elimination of the bridging group and the resulting charge-carrier mobility was highly dependent upon the temperature and the tempering time. An optimum for the charge-carrier mobility was found

at 155 °C (4 minutes) and a tempering at 180 °C (1 minute) The charge-carrier mobility was then around 0.02 $cm^2 V^{-1} s^{-1}$ at an on/off ratio of 10^5.

The temperature for the elimination of the bridging group can be further lowered by the introduction of acid-labile protecting groups on the nitrogen atom, for example, the *tert*-butoxycarbonyl (Boc) group. So, *N*-sulfinyl-*tert*-butylcarbamate was used as dienophile for the reaction with pentacene.[15] The resulting pentacene precursor is shown in Figure 5 (left). If this precursor compound is mixed with a photoacid before film formation (spin coating), protons can be released in the film by UV irradiation that accelerate the elimination of the bridging group through deprotection of the nitrogen atom. In this way the elimination temperature could be lowered from 150 to 130 °C (5 minutes). In OFETs with pentacene layers prepared in this way Hamers and co-workers achieved a charge-carrier mobility of 0.13 $cm^2 V^{-1} s^{-1}$ at an on/off ratio of 3×10^5. At the same time, the possibility of photostructuring semiconductors is opened up. By using photolithographic masks, acid is generated only in the irradiated areas of the film. By selective conversion of the irradiated area the remaining, soluble precursor can be dissolved out of the unirradiated areas (in analogy to the wet chemical development of a negative resist).

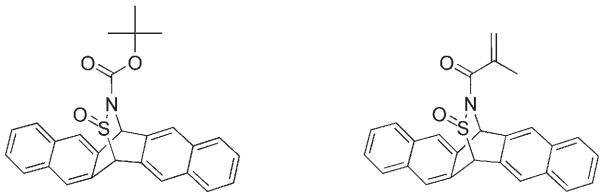

Figure 5. Further pentacene precursors with sulfinylamide bridges.

Structuring of the pentacene film can also be realized by the use of polymerizable bridging groups, for example, in a pentacene precursor with *N*-sulfinylmethacrylamide bridges.[16] This pentacene precursor is also shown in Figure 5 (right). It has good solubility in chlorinated solvents, acetone, and tetrahydrofuran (THF) as well as in esters such as propylene glycol methyl ether acetate (PGMEA). The methylacrylamide group of the bridge can be "polymerized" photochemically. By dissolving out the non-cross-linked precursor from the unirradiated areas and subsequent tempering, a structured pentacene layer is obtained in which, however, the cleaved polymer (polymethacrylamide) remains. The maximum OFET charge-carrier mobility in the bottom-gate configuration with silicon oxide as insulator and gold source and drain electrodes was 0.015 $cm^2 V^{-1} s^{-1}$ in the linear region and 0.021 $cm^2 V^{-1} s^{-1}$ in the saturation region with an on/off ratio of 2×10^5.

An alternative possibility for solubilization of pentacene is afforded by substitution of the primary structure with solubilizing side groups. As direct substitution of the arene with flexible alkyl chains disturbs the π–π interaction between the pentacene units in the solid state, Anthony et al. introduced substituted ethynyl groups in the 6- and 13-positions. These groups can be further substituted by alkyl or trialkylsilyl groups (Figure 6).[17] The synthesis starts with pentacene-6,13-quinone, which is reacted in the first step with alkynyl Grignard reagents and subsequent reduction of the intermediate by $SnCl_2$/HCl to form the pentacene derivative (Scheme 3).

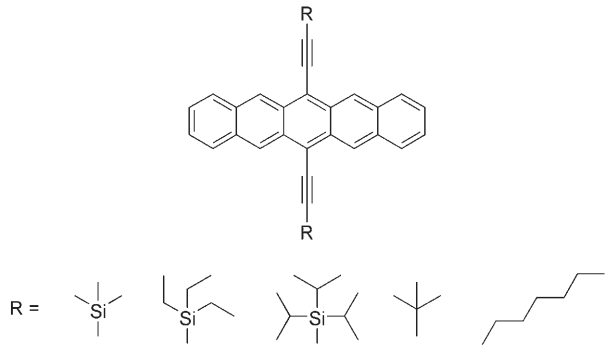

Figure 6. Ethynyl-functionalized, soluble pentacenes.

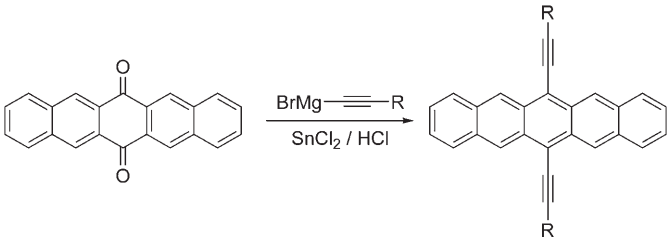

Scheme 3. Synthesis of alkynyl-substituted pentacenes.

Introduction of the alkynyl side groups allows optimal intermolecular π–π interaction of the substituted pentacenes in the solid state. In the solid-state unsubstituted pentacene has a so-called "herringbone" structure with an "edge-on-surface" configuration of the molecules, through which a close electronic interaction with only every second neighboring molecule is possible (Figure 7a). The alkynyl side groups force the pentacenes into a stacked surface-on-surface configuration, which reinforces the π–π interaction between direct neighbors.[18] The size of the (preferably spherical) substituents on the alkynyl side group (e.g. *tert*-butyl, trialkylsilyl) is pivotal to the solid-state structure. Anthony et al. found that the electronic interaction of the pentacene molecules is greatest when the size of the substituents on the pentacene corresponds to about half the length of the pentacene molecule (7 Å). If the substituent is smaller than 7 Å (e.g. triethylsilyl, 6.6 Å), the pentacene molecules in the film form a one-dimensional columnar arrangement (Figure 7b). With triisopropylsilyl (7.5 Å) as substituent, a two-dimensional "brick-wall" arrangement of the pentacenes is found (Figure 7c), whereas with substituents significantly larger than 7 Å a one-dimensional columnar arrangement is again found. A clear correlation between solid-state structure and charge-carrier mobility emerges from this study, whereby the charge-carrier mobility μ_{FET} is a maximum for compounds with "two-dimensional" electronic interaction (e.g.,

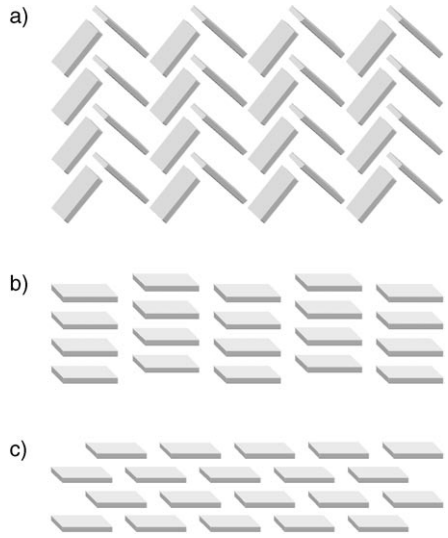

Figure 7. Arrangement of pentacenes in the solid state: a) "herringbone" arrangement in unsubstituted pentacenes; b) one-dimensional columnar arrangement of alkynyl-substituted pentacenes; c) two-dimensional "brick-wall" arrangement of alkynylsilyl-substituted pentacenes.

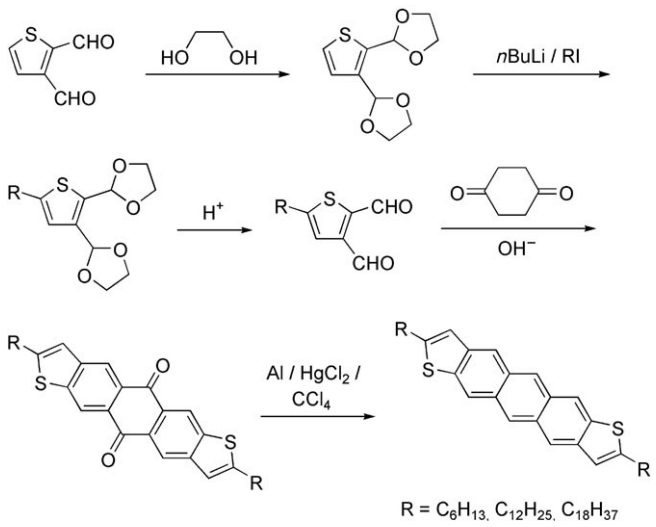

Scheme 4. Synthesis of terminally alkyl-substituted anthradithiophenes (only the *anti* compound is shown).

$0.4\ cm^2V^{-1}s^{-1}$ for (triisopropylsilyl)ethynyl-substituted pentacene, on/off ratio 10^6). Significantly smaller hole mobilities ($<0.001\ cm^2V^{-1}s^{-1}$) were found for compounds with one-dimensional columnar arrangement of the pentacenes (e.g., (triethylsilyl)ethynyl-substituted derivatives). The measurements were carried out on bottom-gate OFETs (gate of highly doped silicon with thermally grown silicon dioxide as insulator (dielectric)). The SiO_2 dielectric was treated with octadecyltrichlorosilane (silanized) before the application of the pentacene layer. In this series of investigations, the pentacene compounds were vapor-deposited as a 75-nm-thick layer. Gold source and drain electrodes were attached after application of the pentacene, although solution processing of the semiconductor is also possible.

The so-called anthradithiopenes (ADT) are isoelectronic with pentacenes. Katz and co-workers synthesized terminally alkyl substituted anthradithiophenes in a multistage synthesis (Scheme 4).[19] The synthesis starts from thiophene-2,3-dicarbaldehyde, which is first protected as the bisacetal. The protected compound is then lithiated in the 5-position with *n*-butyllithium and alkylated with an alkyl iodide. The authors used hexyl, dodecyl, and octadecyl iodide as alkyl iodides. The bisacetal is then deprotected under acidic conditions, and the alkyl-substituted dialdehyde is treated with cyclohexane-1,4-dione in a fourfold aldol condensation reaction, from which a mixture of *syn*- and *anti*-anthradithiophene quinones is obtained. In analogy to the pentacene synthesis, the quinones can be converted into the dialkyl-substituted ADTs. The compounds are relatively soluble in hot toluene and in 1,2-dichlorobenzene. The OFET charge-carrier mobilities were determined by Katz and co-workers for both vapor and solution-processed dialkylanthradithiophene layers. A bottom-gate/top-contact configuration was used for the vapor-deposited samples, and a bottom-contact configuration for the components prepared from solution (spin coating of 0.2–1% solution in hot chlorobenzene). A maximum charge-carrier mobility (hole mobility) of $0.15\ cm^2V^{-1}s^{-1}$ was measured for the dihexyl derivative of the OFETs with vapor-deposited ADTs. Charge-carrier mobilities of 0.01–$0.02\ cm^2V^{-1}s^{-1}$ were measured for dihexylanthradithiophene layers applied from solution.

As with the pentacenes, the anthradithiophenes can be (trialkylsilyl)ethynyl-substituted on the central aromatic ring.[20] These compounds, investigated by Anthony and co-workers, are shown in Figure 8. As with the substituted

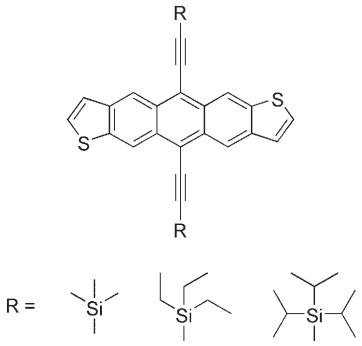

Figure 8. (Trialkylsilyl)ethynyl-substituted anthradithiophenes.

pentacenes, the packing of these molecules in the solid state depends on the substituents, but is more pronounced. The (trimethylsilyl)ethynyl-substituted compound shows the herringbone structure described for the unsubstituted pentacene. Similar to (triisopropylsilyl)ethynyl-substituted pentacene, (triethylsilyl)ethynyl-substituted anthradithiophene forms a two-dimensional layered structure, whereas (triisopropylsilyl)ethynyl-substituted anthradithiophene crystallizes in a one-dimensional columnar structure.

As expected, the solid-state structure again influences considerably the observed charge-carrier mobilities. The compounds were applied from solution (1–2% solutions in

toluene) to bottom-gate OFETs with highly doped silicon as gate, thermally grown silicon dioxide as dielectric, and vapor-deposited gold source and drain electrodes. The highest charge-carrier mobility was obtained with (triethylsilyl)-ethynyl-substituted anthradithiophene (ca. $1\,cm^2V^{-1}s^{-1}$ at an on/off ratio of 10^7). These values even exceeded the characteristic values of OFETs with vapor-deposited (triisopropylsilyl)ethynyl-substituted pentacene as semiconductor, which suggests a very high order of the solution-processed ADT molecules in the film. In contrast, (triisopropylsilyl)-ethynyl-substituted anthradithiophene showed a very low charge-carrier mobility of less than $10^{-4}\,cm^2V^{-1}s^{-1}$ (on/off ratio of 10^3), and no significant FET properties at all were observed for the (trimethylsilyl)ethynyl-substituted anthradithiophene.

An interesting approach in the area of solution-processable oligoacenes was described in 2005 by Blanchard and coworkers with the synthesis of a thiophene–acene "hybrid compound" based on a bis(naphtho[2,3-*b*]thienyl)bithiophene.[21] Trimethylsilyl groups on the central thiophene rings act as solublizing agents in the soluble precursor compound and could be cleaved again with tetrabutylammonium fluoride in pyridine. The synthesis of the precursor compound is shown in Scheme 5. Naphtho[2,3-*b*]thiophene is converted into the corresponding stannylated compound in a reaction with *n*-butyllithium and tributylstannyl chloride. This compound is converted into the precursor compound with 5,5′-dibromo-3,3′-bis(trimethylsilyl)-2,2′-bithiophene in a Stille reaction. 5,5′-Dibromo-3,3′-bis(trimethylsilyl)-2,2′-bithiophene is obtained by bromination of 3,3′,5,5′-tetrakis-(trimethylsilyl)-2,2′-bithiophene with *N*-bromosuccinimide (NBS). This compound in turn is prepared in a one-pot reaction from 2,2′-bithiophene by successive reaction with *n*-butyllithium and trimethylsilyl chloride. The "acene–thiophene" hybrid compound obtained after elimination of the trimethylsilyl groups showed a charge-carrier mobility of around $1\times10^{-2}\,cm^2V^{-1}s^{-1}$ in OFETs with a vapor-deposited semiconductor layer. The 2,2′:5′,2″:5″,2‴-quaterthiophene used as comparison showed about a one order of magnitude lower charge-carrier mobility ($2\times10^{-3}\,cm^2V^{-1}s^{-1}$). The latter-described derivatives also have potential for solution processing of the soluble precursor compounds with subsequent elimination of the trimethylsilyl groups in the solid state.

3.1.2. Oligothiophenes

After oligoacenes, oligothiophenes are the most intensively studied class of oligomers for OFET applications. Whereas unsubstituted oligothiophenes are very poorly soluble and therefore difficult to purify and process, alkyl-substituted oligothiophenes are sufficiently soluble to be purified by, for example, column chromatography. Alkyl-substituted oligothiophenes can be either end-group-functionalized (α,ω-functionalization) or side-group-functionalized (β-functionalization).

There are in general numerous methods for the synthesis of oligothiophenes, as illustrated in Scheme 6 for the sexithiophenes. The oldest method is the oxidative coupling of two shorter oligothiophenes with iron(III) chloride.[22] The

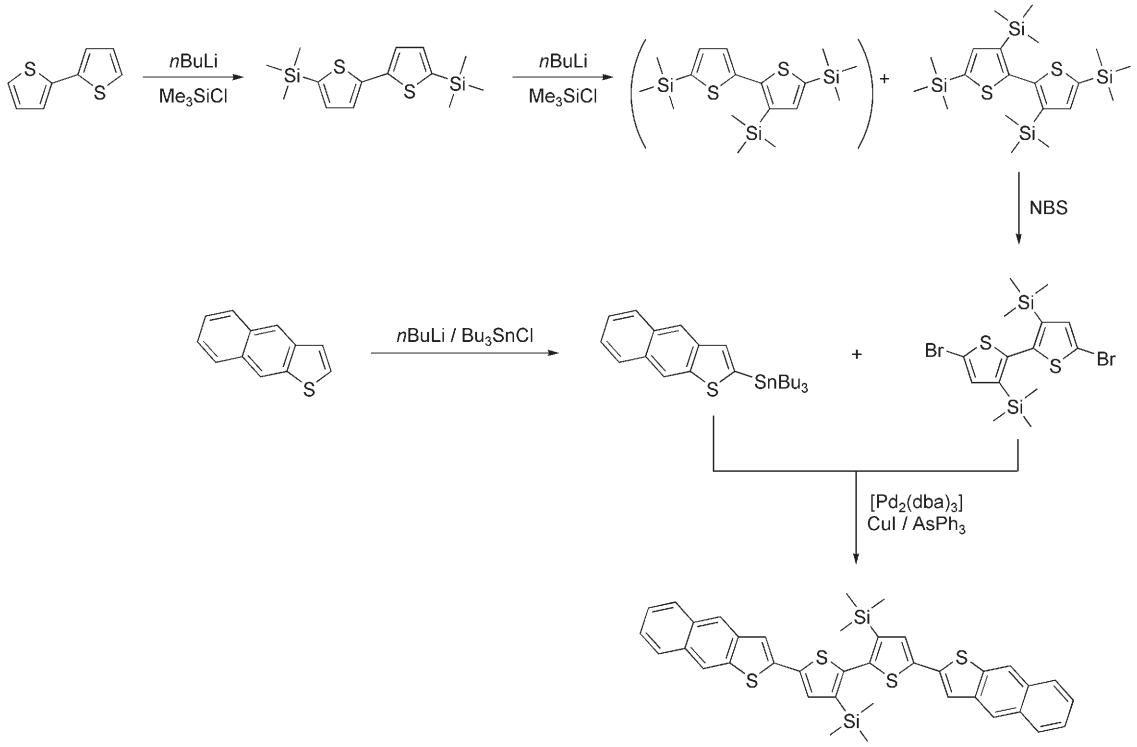

Scheme 5. Synthesis of acene–thiophene "hybrid compounds" (the final elimination of the TMS group is not shown). NBS = *N*-bromosuccinimide.

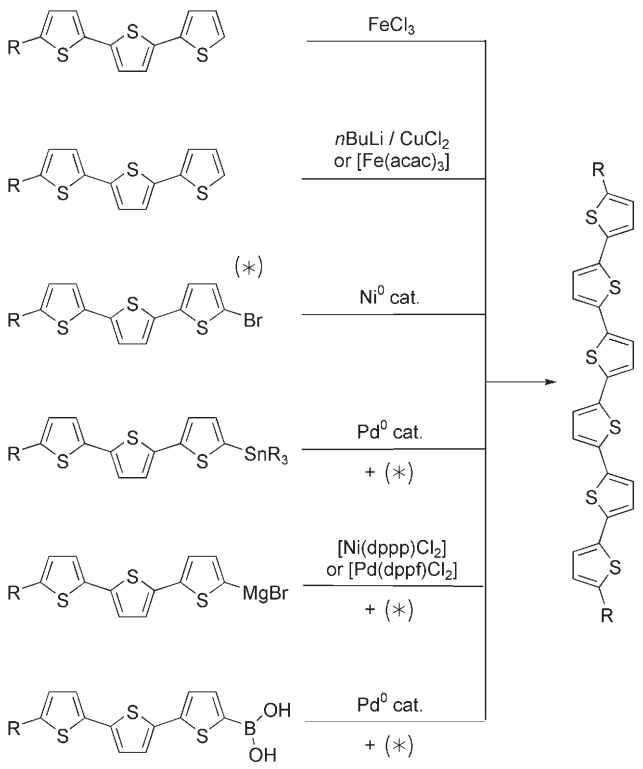

Scheme 6. Possibilities for the synthesis of oligothiophenes, illustrated by the synthesis of sexithiophene (6T).

disadvantage of this synthesis is contamination of the product with iron residues, which often lead to an increase in the "off" current and thus to a lowering of the on/off ratio. An oligomeric mixture is often obtained in this synthesis and can only be separated with considerable effort, especially for unsubstituted starting materials (R = H). In addition, 3-couplings in the oligothiophenes (false coupling) are increasingly found with increasing chain length of the educts.

Such false couplings can be avoided with a transition-metal-catalyzed aryl–aryl coupling reaction. For example, the reactants can first be metalated in the α position with butyl lithium, and then the lithiated compounds can be dimerized with the help of copper(II) chloride or iron(III) acetylacetonate.[23] In addition to the homocoupling of two monobromo-substituted terthiophenes according to Yamamoto, the so-called Kumada coupling, in which a Grignard compound is reacted with a halide, is also a possibility; nickel(II) complexes and palladium(II) complexes (e.g. $[Ni(dppp)Cl_2]$ or $[Pd(dppf)Cl_2]$; dppp = 1,3-bis(diphenylphosphino)propane; dppf = 1,1′-bis(diphenylphosphino)ferrocene) are used as catalysts.[24] In a method introduced by Millstein and Stille in 1978, tin organyls and halides are coupled with the aid of a palladium(0) catalyst.[25] A further transition-metal-catalyzed reaction is the so-called Suzuki coupling, in which a boronic acid or ester is treated with a halide.[26] Again, Pd^0 complexes are used as catalysts, this time under basic conditions.

As discussed in the Introduction, unsubstituted (Scheme 6: R = H) and substituted oligothiophenes show significant differences in solubility and processability.[27] The very low solubility of unsubstituted oligothiophenes can be considerably increased by β substitution (e.g. with alkyl chains). However, the β-alkyl side chains bring about a reduction on the long-range order of the molecules in the solid state, which leads to a reduction in the charge-carrier mobility. The better alternative is a (double) alkyl substitution in the terminal α and ω positions.

α,ω-Dialkyl-functionalized oligothiophenes (Scheme 6: R = alkyl) show a significantly increased OFET charge-carrier mobility relative to unsubstituted compounds in vapor-deposited semiconductor layers. Higher order of the alkyl-substituted oligomers in the film is suggested as a cause of this behavior.[28] Structural analyses by X-ray diffractometry have shown that the terminally alkyl-substituted compounds in the film are arranged perpendicular to the substrate surface (Figure 9), a finding that is supported by the anisotropy of the conductance (the conductance parallel to the substrate surface is higher than the conductance orthogonally). Halik et al. investigated systematically the dependency of the charge-carrier mobility on the number of thiophene units and the length of the alkyl substituents. They compared α,ω-substituted oligomers with four to six thiophene units and alkyl substituents with a chain length between two and ten carbon atoms,[29] and also included differences in the construction of the OFET devices (bottom gate/bottom contact and bottom gate/top contact). They found that the number of thiophene units had only a modest effect on the charge-carrier mobility. In contrast, the charge-carrier mobilities of unsubstituted sexithiophene (6T) and α,ω-dialkyl-substituted sexithiophenes with an alkyl chain length of 2, 6, and 10 show significant differences (Table 1).

The charge-carrier mobilities were higher in both configurations (top contact and bottom contact) for the alkyl-substituted compounds than for the unsubstituted compound 6T. In the top-contact configuration the compounds with the shorter alkyl groups, however, showed significantly higher charge-carrier mobilities than the 6T derivative with the C_{10} side chain, whereas in the bottom-contact configuration the value for the charge-carrier mobility remained essentially independent of the length of the alkyl groups. The highest

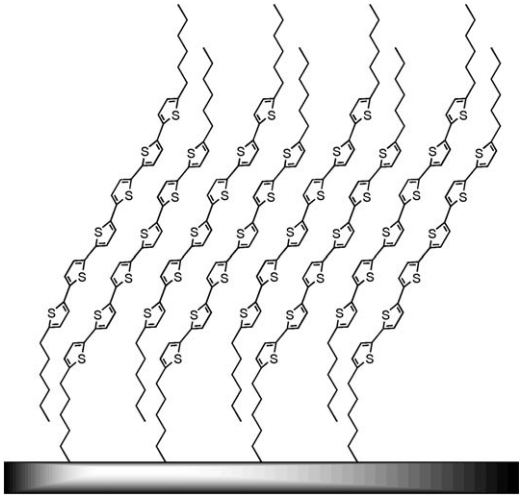

Figure 9. Spatial alignment of α,ω-dialkyl-substituted oligothiophenes in the film relative to the isolator layer.

Table 1: Charge-carrier mobilities of α,ω-dialkyl-substituted oligothiophenes with different length alkyl groups (from Halik et al.[29]).

Semiconductor[a]	Bottom-gate OFETs contact configuration	Charge-carrier mobility [$cm^2V^{-1}s^{-1}$]	on/off ratio
DDα4T	top/bottom	0.1/0.2	10^4/10^5
DDα5T	top/bottom	0.1/0.5	10^4/10^5
DDα6T	top/bottom	0.1/0.5	10^4/10^5
DHα6T	top/bottom	1.0/0.5	10^4/10^3
DEα6T	top/bottom	1.1/0.6	10^4/10^4
6T	top/bottom	0.07/0.1	10^2/10^3

[a] DDα4T = didecylquaterthiophene, DDα5T = didecylquinquethiophene, DDα6T = didecylsexithiophene, DHα6T = dihexylsexithiophene, DEα6T = diethylsexithiophene, 6T = sexithiophene.

charge-carrier mobilities were found for the oligothiophene derivatives with C_2 and C_6 alkyl chains in the top-contact configuration. Halik et al. rationalized this result on the basis of a significantly reduced "barrier" for migration of the charge carrier in the case of the shorter alkyl chains. These differences come into effect to a much greater extent in the top-contact configuration than in the bottom-contact arrangement, since in the former many such "barriers" come into effect when crossing the semiconductor layer.

Solution-processed OFETs with an active layer of α,ω-dialkyl-substituted oligothiophenes can be prepared with a suitable solvent and processing temperature. Garnier et al. showed that the charge-carrier mobility ($1.2\times10^{-2}\,cm^2V^{-1}s^{-1}$) with α,ω-dihexylquaterthiophene as p-semiconductor in solution-processed layers (spin coating from chloroform) was only slightly lower than that of the vapor-deposited films ($3\times10^{-2}\,cm\,V^{-1}s^{-1}$).[30] About a 10 times lower charge-carrier mobility was measured for unsubstituted quaterthiophene ($2.5\times10^{-3}\,cm^2V^{-1}s^{-1}$). Garnier et al. attributed this difference to the liquid crystal properties of their α,ω-dialkyl-substituted oligothiophenes, on the basis of which the molecules in the layer can achieve a higher long-range order.[31]

Katz et al. investigated solution-processed OFETs with α,ω-dihexylquinquethiophene (DHα5T) and α,ω-dihexylsexithiophene (DHα6T) as semiconductors.[32] The compounds were processed into thin films from solutions of the semiconductors in chlorobenzene, 1,2,4-trichlorobenzene, or 3-methylthiophene at 50–60 °C (spin coating). Either thermal silicon dioxide on highly doped silicon (as a gate electrode) or polyimide on indium–tin oxide (ITO) acted as substrates. After removal of solvent residues by heating in a vacuum, the gold source and drain electrodes were applied by vapor deposition (top-contact configuration). Charge-carrier mobilities of up to $0.1\,cm^2V^{-1}s^{-1}$ were measured in the OFETS prepared from DHα6T. DHα5T showed a maximum charge-carrier mobility of $0.04\,cm^{-1}\,V^{-1}s^{-1}$.

The previous results show impressively that it is generally possible to process α,ω-dialkyl-substituted oligothiophenes into OFETs from solution. However, owing to their limited solubility, the oligomers must be processed mostly at high temperatures from high-boiling solvents or by warming the substrate. As already pointed out in the Introduction, one concept for increasing the solubility still further is the synthesis of angularly constructed molecules and of molecules with three-dimensional molecular structure. Ponomarenko et al. describe radial oligothiophenes that were prepared by Kumada coupling of 1,3,5-tribromobenzene with ω-Grignard compounds of α-decyl-substituted oligothiophenes (Scheme 7).[33] The compounds are readily soluble in chloroform and can be processed by spin-coating. In a bottom-gate/bottom-contact configuration Ponomarenko et al. were able to obtain maximum charge-carrier mobilities of 2×

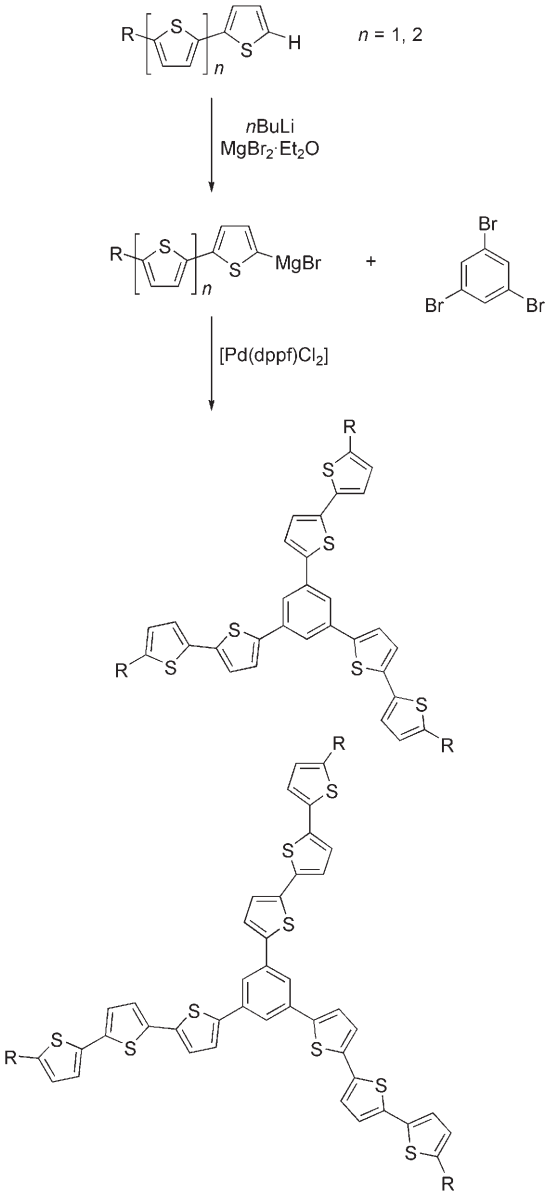

Scheme 7. Synthesis of radial oligothiophenes with a 1,3,5-trisubstituted benzene core segment.

10^{-4} $cm^2 V^{-1} s^{-1}$ for 1,3,5-tris(5″-decyl-2,2′:5′,2″-terthien-5-yl)benzene (on/off ratio 10^2 at a threshold voltage close to 0 V). It emerges from AFM and X-ray measurements that the three-armed molecules arranged themselves into lamellar layers in the film. It may be assumed that strong π–π interactions arise within the layers; between layers the interaction is small, also owing to the extended C_{10} alkyl substituents, which is in agreement with the low OFET charge-carrier mobilities.

Liu et al. replaced the 1,3,5-substituted benzene core of the radial oligothiophenes they had previously synthesized with truxene (10,15-dihydro-5*H*-diindeno[1,2-α;1′,2′-*c*]fluorene), which is hexahexyl-substituted to increase the solubility still further. The side arms comprise one to three thiophene units.[34] The construction of the oligomers starting from tribromotruxene was carried out by repetitive Suzuki coupling with thiophene-2-boronic acid and subsequent bromination of the thiophene side groups in the 5-position with NBS (Scheme 8). The soluble compounds could be processed by spin coating and produced homogeneous, polycrystalline films with different degrees of crystallization. Both X-ray scattering and scanning electron microscopy demonstrated that the morphology of the compounds in the solid state shifts from polycrystalline towards amorphous with increasing number of thiophene units. The highest OFET charge-carrier mobility in the bottom-gate/top-contact configuration was measured at 1×10^{-3} $cm^2 V^{-1} s^{-1}$ for the more crystalline compounds with only one thiophene unit in each side arm.

In another approach Ponomarenko et al. pursued the synthesis of three-dimensional, radial oligothiophenes with flexible alkyl spacers.[35] Starting from a tetragonal silicon center, they attached four hexyl-substituted quaterthiophene arms through flexible alkyl spacer units. The synthetic pathway is shown in Scheme 9. The tetraallylsilyl core unit is obtained by reaction of tetrachlorosilane with allyl magnesium chloride. 5-(Undec-10-en-1-yl)-2,2′-bithiophene is terminally dimethylsilyl-functionalized in a hydrosilylation reaction with 1,1,3,3-tetramethyldisiloxane. This Si–H-functionalized compound is added to the double bonds of the core unit in a further fourfold hydrosilylation reaction. The tetragonal compound with terminal bithiophene units obtained is tetrabrominated with NBS and converted into the radial target compound with 5-hexyl-2,2′-bithiophene-5′-pinacolatoboronate by Suzuki coupling. The crystalline compound is soluble in toluene, THF, and chloroform with slight warming, and homogeneous films can be obtained by spin coating. AFM measurements suggest that the four-armed molecule is arranged in the film perpendicular to the substrate in lamellar layers, similar to α,ω-substituted oligothiophenes, in which each of two side arms are directed upwards and two downwards. In an OFET device in bottom-gate/bottom-contact configuration, a charge-carrier mobility of 1×10^{-2} $cm^2 V^{-1} s^{-1}$ at an on/off ratio of 10^6 was measured for solution-processed layers (spin coating from toluene/tempering at 70 °C). The value for the hole mobility is comparable with that of Halik et al. for α,ω-didecylquaterthiophene.

A further possibility for soluble three-dimensionally constructed oligothiophenes is the synthesis of cruciform compounds with flexible molecular structure (so-called "swivel cruciforms") whose subunits are rotatable about the central molecular axis, unlike the previously described radial compounds with 1,3,5-trisubstituted benzene or truxenes as rigid core. This behavior is expressed by the term "swivel". Farrell, Scherf, and co-workers described different swivel-cruciform oligothiophenes with, in each case, three to seven thiophene units in a molecular arm, in part with additional α,ω-alkyl substituents.[36] In the synthesis, 3,3′-bithiophene as core segment is first tetrabrominated in the 2,2′,5,5′-position and then coupled fourfold with α-functionalized oligothiophenes by Stille coupling (Scheme 10). The α,ω-dihexylpentathiophene dimer (R = hexyl, $n = 2$) is particularly soluble in chloroform. X-ray diffractometric investigations on layers produced by spin

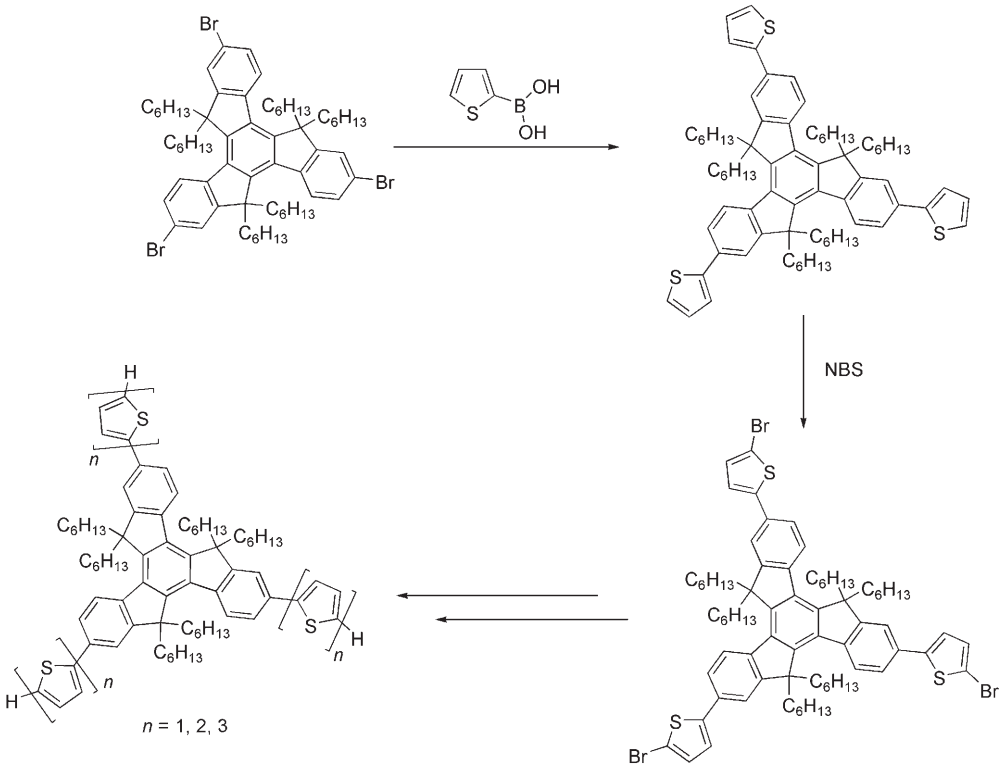

Scheme 8. Synthesis of radial oligothiophenes with a truxene core segment.

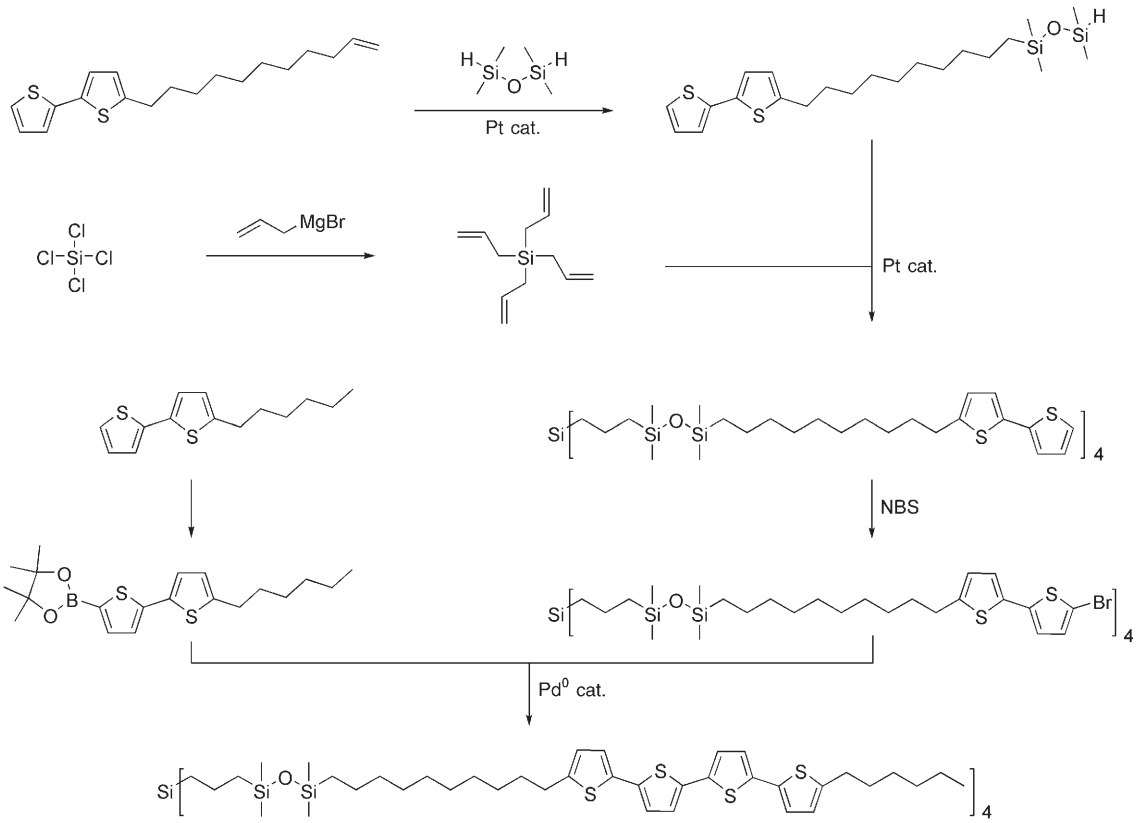

Scheme 9. Synthesis of radial oligothiophenes with a tetragonal SiR_4 core segment.

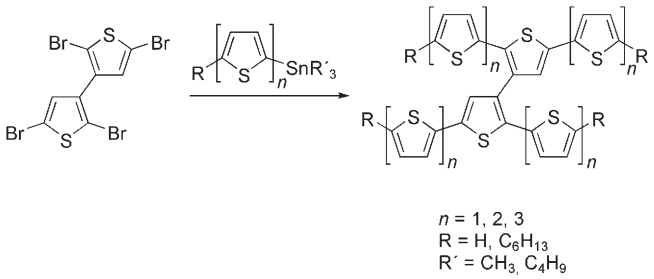

Scheme 10. Synthesis of "swivel-cruciform" oligothiophenes.

coating suggest that similar to their linear analogues, the dimeric molecules are arranged perpendicular to the substrate in lamellar stacks. The OFET properties were investigated in devices with bottom-gate/bottom-contact configuration. The semiconductor layer was applied by spin coating from chloroform and tempered at 120°C for subsequent crystallization. A maximum charge-carrier mobility of $1.2 \times 10^{-2}\,cm^2\,V^{-1}\,s^{-1}$ with an on/off ratio of $> 10^5$ was found. This value lies in the same order of magnitude as the charge-carrier mobility of vapor-deposited layers of linear α,ω-alkyl-substituted oligothiophenes. Oligothiophene dimers with a spiro linkage to the core unit have also been described as an alternative to the swivel-cruciform oligothiophenes discussed.[37]

The use of soluble precursor compounds for pentacene derivatives has already been discussed in detail in Section 3.1.1. Fréchet and co-workers extended this concept to oligothiophenes.[38] They prepared oligothiophenes with four to seven thiophene units substituted in the α,ω-position with 1-carboxypropyl groups. These groups can be cleaved thermally (ester pyrolysis) to produce insoluble α,ω-propenyl-substituted oligothiophenes (Scheme 11).

The synthesis of these oligothiophenes is shown in Scheme 12. First, 2,2′-bithiophene is treated with propanoyl chloride in a Friedel–Crafts acylation. The ketone obtained is reduced to the secondary alcohol with $LiAlH_4$ and esterified with 2-butyloctanoyl chloride. The functionalized bithio-

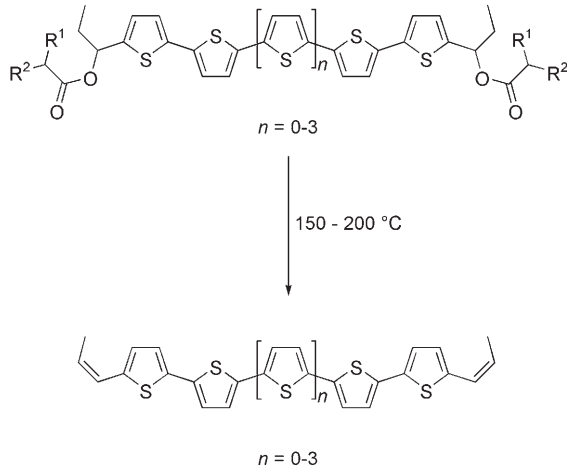

Scheme 11. Thermal conversion of α,ω-bis(1-carboxypropyl)-substituted oligothiophenes.

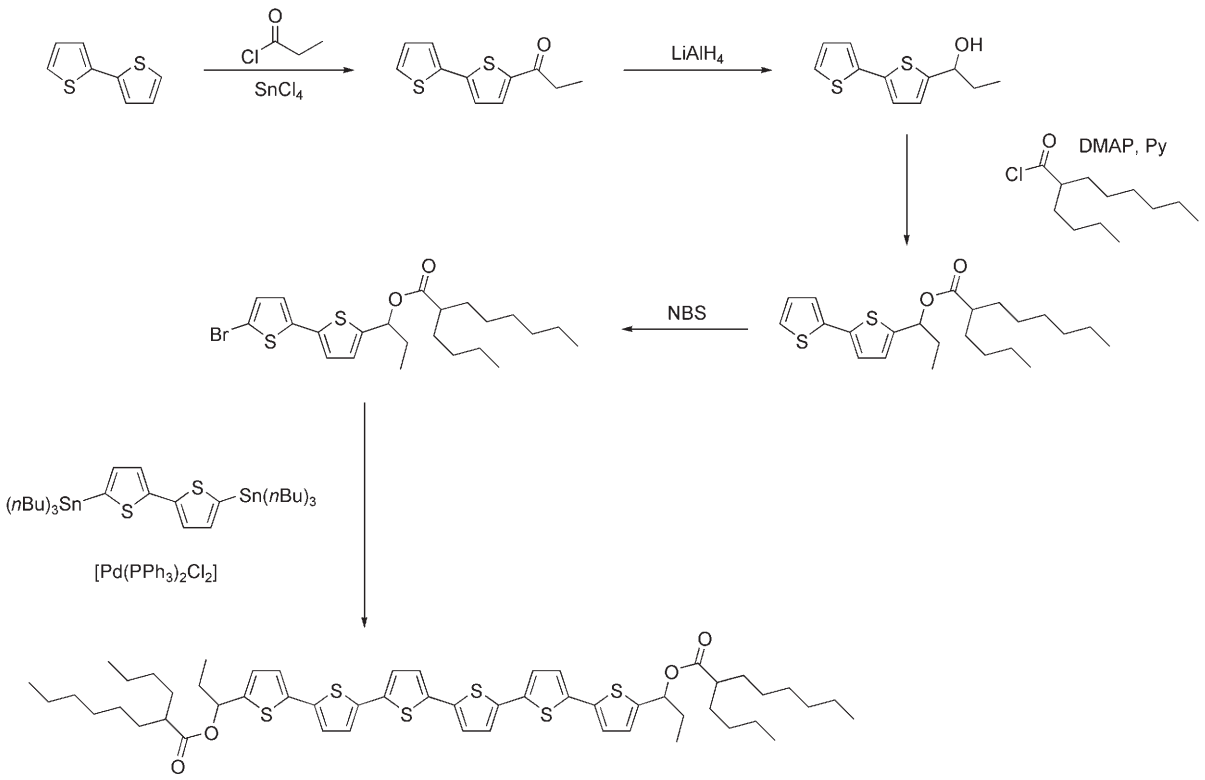

Scheme 12. Synthesis of α,ω-bis(1-carboxypropyl)-substituted oligothiophenes, illustrated by the example of the sexithiophene derivative. DMAP = 4-dimethylaminopyridine; Py = pyridine.

phene is brominated with NBS and converted into the target oligomers. The synthesis of the quaterthiophene derivatives is carried out by homocoupling of the bithiophene. The quinquethiophene derivative and the sexithiophene derivative are obtained by Stille coupling of the brominated bithiophene with respectively 2,5-bis(trimethylstannyl)thiophene and 5,5′-bis(trimethylstannyl)-2,2′-bithiophene. In the synthesis of the heptathiophene derivative, the brominated bithiophene is first extended by one thiophene unit by Stille coupling with 2-trimethylstannylthiophene, again brominated in the ω position and treated with 2,5-bis(trimethylstannyl)-thiophene.

Fréchet and co-workers carried out the thermal cleavage of the ester groups in the film and followed the associated changes in morphology with NEXAFS (near-edge X-ray absorption fine structure) spectroscopy and AFM (atomic force microscopy).[38c] Oligomer films were applied by spin coating onto SiO_2 supports from chloroform and then heated at different temperatures. The quaterthiophene derivative did not form a homogeneous film and could not be examined further. The quinque- and sexithiophene derivatives formed homogeneous amorphous films at room temperature. The cleavage of the solubilizing ester groups starts at around 125 °C and is almost complete at 200 °C. The thermal cleavage of the ester groups is associated with a considerable reorganization of the molecule in the solid state. Terrace structures are formed during the thermal conversion, whereby the molecular axis is oriented perpendicular to the substrate. Films of the quinquethiophene derivatives remain uniform up to around 225 °C; only on increasing the temperature to 250 °C were cracks and de-wetting observed. The films of sexithiophene showed cracks only above 250 °C. In contrast to the shorter oligomers, reorientation of the molecules (terrace formation) for the heptathiophene derivative was only observed above 225 °C. The authors attributed these results to competitive influencing factors that drive the reorientation of the molecules in the film. These are the intermolecular π–π interactions between the conjugated oligomers and the interactions with the substrate. At the temperatures necessary for the cleavage of the ester groups, the kinetic energy necessary for the reorientation is supplied simultaneously to the molecules. The reorientation takes place even at lower temperatures for the smaller oligomers (quinque- and sexithiophene derivatives). This leads to an increased kinetic energy of the molecules at a further increase in temperature so that the interaction energy with the substrate can be more readily overcome. In the heptathiophene derivative cleavage and reorientation only take place above 300 °C

Measurements of the dependency of OFET charge-carrier mobility on conversion temperature in the solid state show a good correlation with the observed morphology in the film. The measurements were carried out on OFETs with Si gate, thermal SiO_2 as dielectric, and gold source and drain electrode in the top-contact configuration. Whereas the charge-carrier mobilities μ_{FET} at room temperature were in all cases around $10^{-5}\,cm^2\,V^{-1}\,s^{-1}$, significantly higher μ_{FET} values were measured after elimination of the ester group: for the quinquethiophene derivative a maximum value of $0.02\,cm^2\,V^{-1}\,s^{-1}$ at an on/off ratio of 10^4 (tempering at 200 °C). After a further temperature increase to 225 °C the

μ_{FET} values fall again rapidly. The sexithiophene derivative shows maximum μ_{FET} values of 0.05 $cm^2V^{-1}s^{-1}$ (tempering at 200 °C), whereas a maximum charge-carrier mobility of 0.06 $cm^2V^{-1}s^{-1}$ is first achieved above a conversion temperature of 225 °C for the heptathiophene derivative.

Fréchet et al. have tested different substrates and application methods for the semiconductor layers, in particular for the sexithiophene derivative. No uniform film could be produced for both silanized SiO_2 (octadecyltrichlorosilane (OTS) as silylation reagent) and for poly(vinylphenol) (PVP) as polymeric dielectric, independent of the solvent used. Spin coating, dip coating, and inkjet printing were compared as application methods. The best result was achieved after spin coating from chloroform and with untreated thermal SiO_2 as dielectric in the top-contact configuration (charge-carrier mobility μ_{FET}: 0.07 $cm^2V^{-1}s^{-1}$). The high charge-carrier mobility of OFETs in the bottom-contact configuration prepared by inkjet printing from anisole solution is attractive for potential roll-to-roll applications. At 0.06 $cm^2V^{-1}s^{-1}$, this value almost approaches that obtained by spin coating, so that inkjet printing represents a very promising processing variant.

A general disadvantage of oligothiophenes is their high sensitivity towards atmospheric oxygen. As already discussed in the Introduction, the oxidation stability of the compounds can be increased by a reduction in the HOMO energy level. In the case of oligothiophenes, this can be achieved through the introduction of fluorene units as "chain components". Strohriegl and co-workers prepared 5,5′-bis(9,9′-dialkylfluoren-2-yl)-2,2′-bithiophene oligomers and determined their OFET charge-carrier mobilities.[39] They tested two different synthetic routes for the oligomers with different lengths of the alkyl substituent R (Scheme 13): in both cases a Suzuki coupling is involved in which in Route 1 the 2-boronic ester of a 9,9-dialkylfluorene is treated with 5,5′-dibromo-2,2′-bithiophene, and in Route 2 2-bromo-9,9-dialkylfluorene with the diboronic ester of the bithiophene. Whereas the reaction in Route 1 leads to a series of by-products (e.g. dimers through homocoupling), the reaction according to Route 2 leads to the target oligomer within 2 hours in very good yield (75 %).

Differential calorimetric and polarization microscopic investigations show that the oligomers with linear alkyl side groups (e.g. ethyl, butyl, octyl) are crystalline, whereas compounds with branched alkyl side groups (e.g. methylpropyl, ethylhexyl) are amorphous. Some of the oligomers were tested as the semiconductors in OFETs with bottom-gate/bottom-contact configuration. Highly doped n-silicon acted as the gate electrode, on which thermally grown silicon dioxide was used as insulator. The gold source and drain electrodes were then attached, followed by the fluorene–thiophene oligomers as a 100-nm-thick layer. Finally, the devices were tempered for 20 minutes at 80 °C. A charge-carrier mobility of 10^{-5} $cm^2V^{-1}s^{-1}$ at an on/off ratio of 10^4 was measured for R = methylpropyl. Since this compound is amorphous and has very good film formation properties, similar charge-carrier mobilities were also achieved for solution-processed OFETs. In contrast, the crystalline oligomers with R = ethyl or butyl do not allow solution processing. A charge-carrier mobility of 2×10^{-4} $cm^2V^{-1}s^{-1}$ (on/off ratio 10^4) was measured for the butyl-substituted oligomer for OFETs with a vapor-deposited semiconductor layer. The highest charge-carrier mobility of 3×10^{-3} $cm^2V^{-1}s^{-1}$ was demonstrated for the highly crystalline tetraethyl derivative (on/off ratio of 10^6).

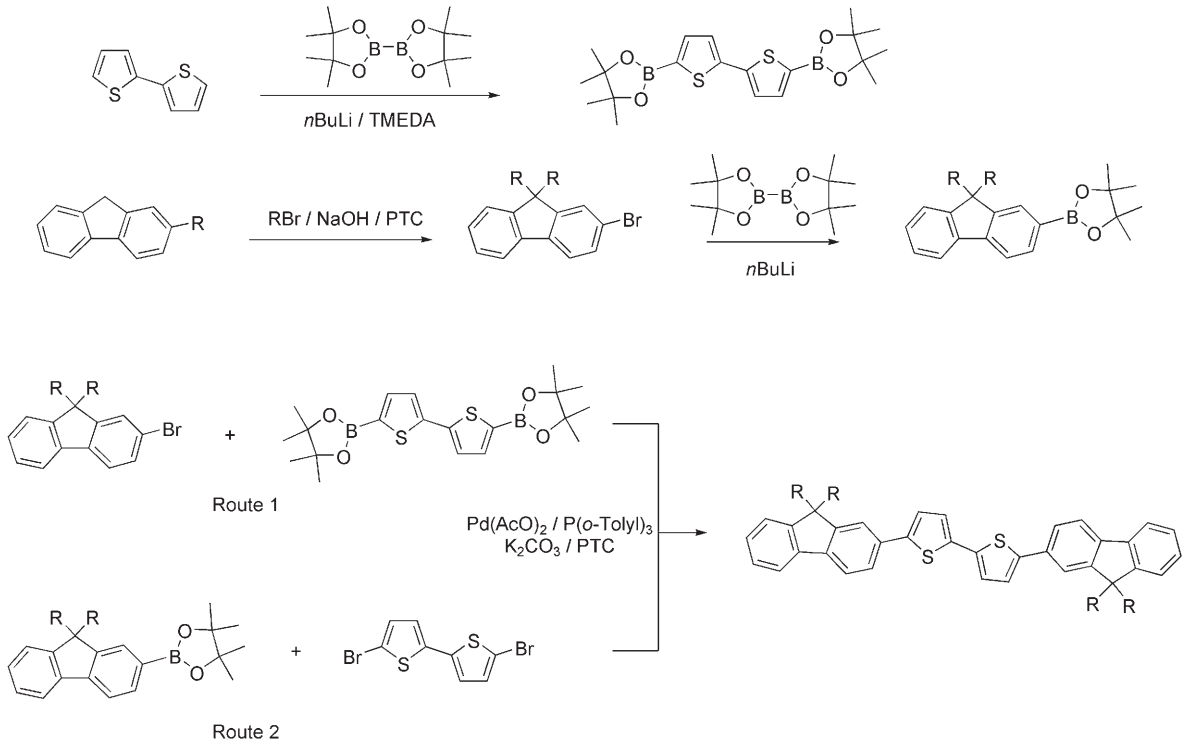

Scheme 13. Synthetic pathways to 5,5′-bis(9,9′-dialkylfluoren-2-yl)-2,2′-bisthiophenes (R = ethyl, butyl, octyl, methylpropyl, ethylhexyl). TMEDA = *N*,*N*,*N*′,*N*′-tetramethylethylenediamine; PTC = phase-transfer catalyst.

The stability of the OFETs with the tetraethyl oligomer as semiconductor was tested by storage of the components for three months under ambient conditions. The properties of the OFET devices and directly after preparation and after three-month storage under ambient conditions are compared in Figure 10. Both the charge-carrier mobility and the on/off ratio remained almost constant. The threshold voltage was shifted from −15 V for the "freshly" prepared component to only −5 V after storage.

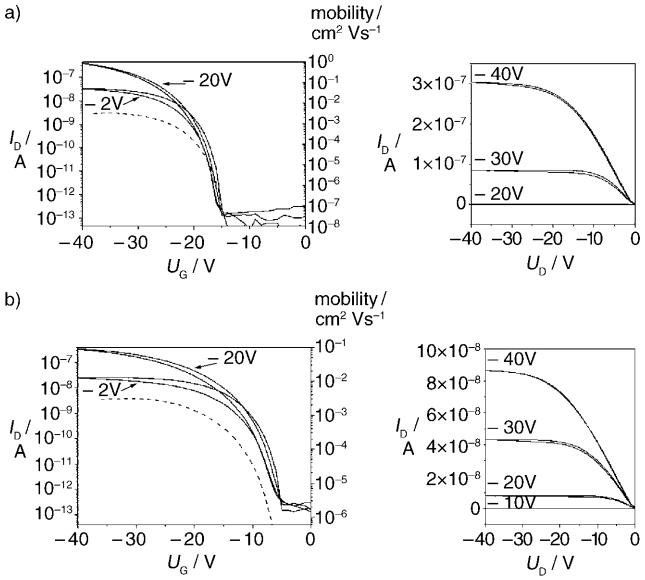

Figure 10. OFET characteristic plots for bottom-gate/top-contact devices with 5,5′-bis(9,9′-diethylfluoren-2-yl)-2,2′-bithiophene as oligomeric semiconductor: a) freshly prepared device; b) after storage for 3 months under ambient conditions. Left: OFET transfer characteristics (solid lines, $U_D = -2$ V, −20 V). The dashed curves show the mobility values (for $U_D = -2$ V). Right: Output characteristics for different gate voltages.

Materials of the same substance class but without alkyl chains at the 9,9′-positions of the fluorene units show a charge-carrier mobility in the region of 0.1 $cm^2 V^{-1} s^{-1}$ if they are applied to a tempered substrate by vacuum sublimation and if a top-gate OFET configuration is chosen instead of the bottom-gate configuration.[40] With solution processing by spin coating, these poorly soluble materials lose about two orders of magnitude in their charge-carrier mobilities since it is then very difficult to produce homogeneous, microcrystalline films.

3.1.3. ***Liquid Crystals***

The work on the application of low molecular weight OFET materials described previously clearly shows that the macroscopic orientation of the molecules in the film plays the pivotal role for the charge-carrier mobility that is achievable. Therefore, it followed that high order could also be achieved with liquid-crystalline compounds. Initial time-of-flight (TOF) measurements of charge-carrier mobility in discotic liquid crystals had already been described in 1994 by Ringsdorf and co-workers. 2,3,6,7,10,11-Hexa(hexylthio)triphenylene showed TOF charge-carrier mobilities of up to 0.1 $cm^2 V^{-1} s^{-1}$, although it has to be taken into account that OFET charge-carrier mobilities generally turn out to be lower.[41]

Garnier et al. and Amundson et al. later carried out experiments in liquid-crystalline α,ω-dialkyl-substituted oligothiophenes.[42] Unlike the discotic compounds investigated by Ringsdorf and co-workers, these are calamitic (rod-shaped) liquid crystals. The compounds, crystalline at room temperature, form one or more thermotropic liquid-crystal phases (LC phases). Supramolecular assembly of the molecules in the solid state can be conveniently accomplished from nematic or smectic LC phases with or without the use of an additional orientation layer. McCulloch et al. tested the suitability of liquid-crystalline α,ω-substituted oligothiophenes with cross-linkable α,ω-substituents for their suitability as semiconductors in OFETs.[43] The idea behind this approach is an orientation of the non-cross-linked compounds in the LC state followed by a final structural fixing of the ordered state by photochemical cross-linking. The quaterthiophene derivatives illustrated in Figure 11 were used for this purpose. Maximum charge-carrier mobilities between 1×10^{-4} and 2×10^{-3} $cm^2 V^{-1} s^{-1}$ were measured for the quaterthiophenes in the cross-linked state.

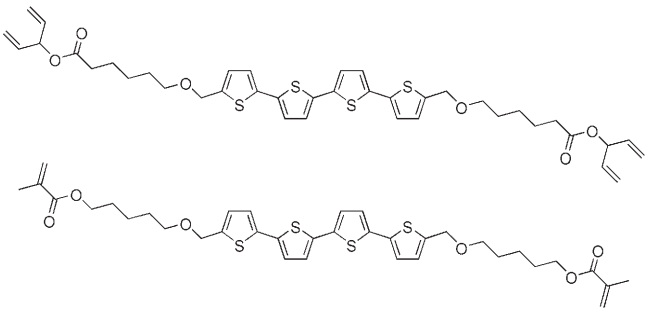

Figure 11. Cross-linkable, liquid-crystalline oligothiophenes.

OFETs in the bottom-gate/bottom-contact configuration with thermal silicon dioxide as gate dielectric and gold source and drain electrodes were used for the measurement of the charge-carrier mobilities. The SiO_2 surface was treated (silanized) with hexamethyldisilazane (HMDS) to ensure a perpendicular orientation of the molecular axis relative to the substrate in the smectic LC phase. For the orientation, the semiconductor layers were heated to a few degrees above the isotropization temperature and then slowly cooled into the LC phase. The layers were finally cross-linked photochemically by UV irradiation. The charge-carrier mobilities were measured before and after orientation as well as after cross-linking. The values for the charge-carrier mobilities are slightly improved after tempering (orientation) relative to the values before tempering, but fell again after cross-linking. McCulloch et al. attributed the small orientation effect to the high viscosity in the film through which an optimal alignment of the molecules is made difficult.

Liquid-crystalline bis(thienylethynyl)-substituted terthiophene derivatives (Figure 12) were also investigated in addition to the quaterthiophene derivatives.[44] Mobilities of up to 0.02 $cm^2 V^{-1} s^{-1}$ were reported for this class of molecules.

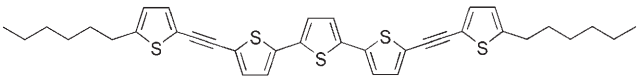

Figure 12. Structure of a liquid-crystalline 5,5″-bis(5-hexyl-2-thienylethynyl)-2,2′:5′,2″-terthiophene.

These oligothiophenes exhibit very high stability towards humidity and oxygen as well as very good solubility in common solvents. The high mobilities are explained by the formation of extended liquid-crystal domains in the semiconductor layer.

A very interesting group of organic semiconductor materials are soluble discotic liquid-crystalline compounds. The interest is traced back to the work of Ringsdorf and coworkers described previously. Building on this work, Müllen and co-workers achieved higher degrees of order and charge-carrier mobilities through an increase in the intermolecular interactions within the columns, for example, by use of extended π-electron systems as core segment of the discotic molecules. This strategy was particularly successful for hexa-*peri*-benzocoronenes (HBCs) with solubilizing side chains at the periphery. Müllen and co-workers devised a simple and very efficient synthetic route for their preparation. Thus, correspondingly substituted hexaphenylbenzenes as HBC precursors are subjected to an oxidative cyclodehydrogenation (e.g. with $FeCl_3$ or $AlCl_3$/Cu salt; Scheme 14).[45]

Correspondingly substituted HBCs thermotropically develop liquid-crystalline phases in which the molecules take up columnar superstructures, which in turn can form two-dimensional lattices. The extended π orbitals of neighboring molecules overlap optimally in the mesophase so that in microwave conductance experiments very high microscopic (intercolumnar) charge-carrier mobilities of up to 1.1 $cm^2 V^{-1} s^{-1}$ (for HBC-PhC_{12}) were measured along the columnar axis.[46] For effective application in OFETs, the HBC molecular discs must be aligned heterotropically, that is, perpendicular to the substrate, since charge transport has to take place through the columns. Two methods were developed to realize such a morphology: spin coating onto silanized (hydrophobic) oxidic substrates and so-called zone casting.[47] In the latter method, a solution of the semiconductor is applied through a jet onto a moving substrate whereby the temperature of the jet and the substrate can be accurately controlled. In bottom-gate OFETs, charge-carrier mobilities of up to 1×10^{-2} $cm^2 V^{-1} s^{-1}$ (on/off ratio 10^4) were measured for HBC layers ($R = C_{12}H_{25}$) applied by zone casting.[48]

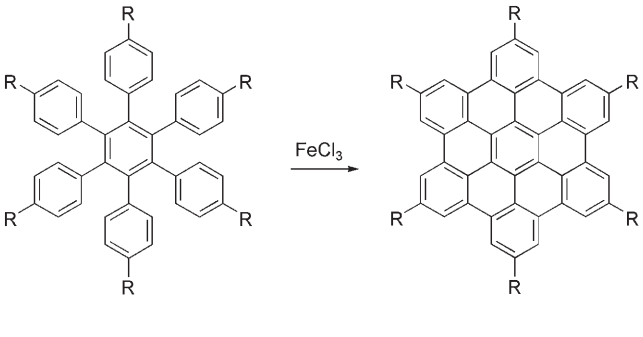

Scheme 14. Synthetic pathways to the preparation of hexa-*peri*-benzocoronenes by oxidative cyclodehydrogenation.

3.2. Polymeric Materials

3.2.1. Polythiophenes

Arguments for the use of soluble, semiconducting polymers in microelectronic devices (including OFETs) are their simple processability, normally very good film-forming properties, and the high flexibility of the films relative to many low molecular weight compounds. So-called "small molecules" can be processed both by means of gas-phase techniques and from solution, as discussed in detail in Section 3.1. However, the resulting polycrystalline films are often very susceptible to mechanical stress. With a view to polymeric semiconductors, polythiophenes combine attractive semiconductor characteristics (very low "off" conductance, high field-induced charge-carrier mobility in the "on" state) with typical polymer properties such as flexibility and low specific mass. Owing to their good synthetic accessibility, polythiophenes are currently one of the most investigated and most frequently used material classes of π-conjugated polymers for OFET devices.

Chemical and electrochemical methods were used for the preparation of the first, unsubstituted polythiophenes. The first chemical syntheses were published in 1980 by the groups of Yamamoto and Lin (Scheme 15).[49] The minor, soluble

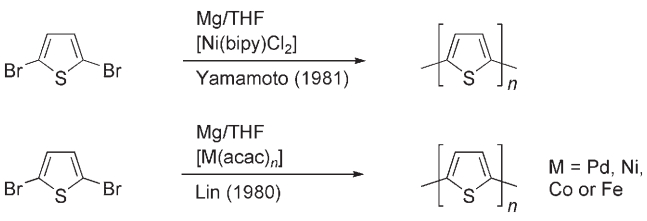

Scheme 15. First chemical syntheses of unsubstituted polythiophenes. bipy = 2,2′-bipyridyl; acac = acetylacetonate.

fraction of the products obtained has a number average molecular weight (M_n) of less than 3000 $g\,mol^{-1}$, which corresponds to a coupling of up to 36 thiophene rings. The main fraction (ca. 80%) is, however, insoluble. Field-effect transistors with unsubstituted polythiophene as semiconductor material were described for the first time by Ando and coworkers in 1986. A charge-carrier mobility $\mu_{FET,sat}$ of approximately 1×10^{-5} $cm^2 V^{-1} s^{-1}$ with an on/off ratio of 100–1000 was found for a bottom-gate transistor.[50] The low solubility of the unsubstituted polythiophenes is problematic. Alkyl chains were introduced into the 3-position of the thiophene monomers to produce longer chain, more readily

soluble, and, above all, morphologically more uniform polythiophene layers. Soluble poly(alkylthiophene)s were reported for the first time in 1985. It was shown that the alkyl side chains must contain at least four carbon atoms for sufficiently soluble polythiophenes to be obtained. The first poly(alkylthiophene)s were prepared in a Kumada metal-catalyzed cross-coupling reaction. The molecular weights achieved were still relatively low ($M_n = 3000$–$8000\ g\,mol^{-1}$).[51] Poly(hexylthiophene) (PHT) was synthesized by Sugimoto et al. by oxidative polymerization of 3-hexylthiophene with $FeCl_3$ (see also Scheme 16a).[52] The polymer films applied from chloroform had a low OFET charge-carrier mobility of 10^{-5}–$10^{-4}\ cm^2\,V^{-1}\,s^{-1}$.[53]

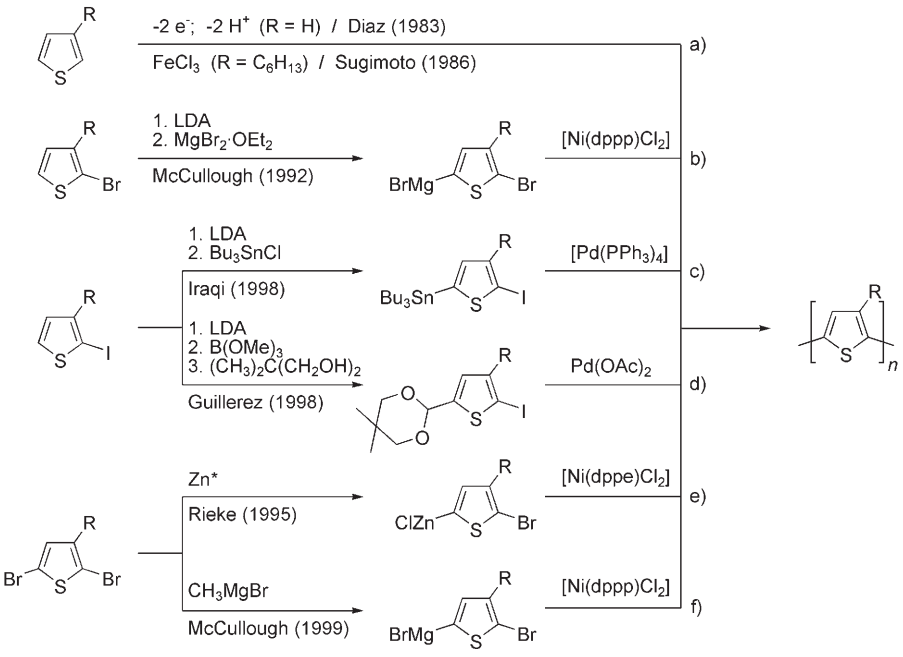

Scheme 16. Synthetic strategies for the preparation of regioirregular (a) and regioregular poly(alkylthiophene)s (b–f); only one organometallic intermediate is illustrated in each case for routes (e) and (f). (See reference [52] and references therein.)

Since 3-alkylthiophenes are not mirror symmetric monomers, there are three possible coupling patterns of dimeric subunits in the polymer chain if the thiophene building blocks are connected solely in the 2- and 5-positions (Figure 13). These are a 2,5′- or head-to-tail coupling (called "HT"), a 2,2′- or head-to-head coupling ("HH"), and a 5,5′- or tail-to-tail coupling ("TT").

Regioirregularly constructed poly(alkylthiophene)s (P3ATs) have a more or less random distribution of HT, HH, and TT couplings. Owing to the extensive twisting of the polymer chains in the sterically demanding HH couplings, the

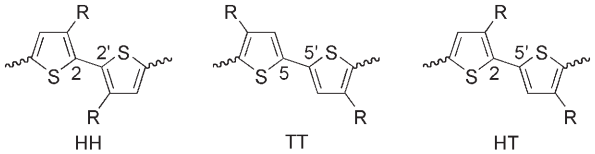

Figure 13. Regioisomeric coupling patterns in poly(alkylthiophene)s.

intramolecular electronic conjugation in the chain and the possibility for intermolecular interaction in the solid state is limited. It was therefore a considerable synthetic challenge to develop preparative routes for regioregular poly(3-alkylthiophene)s with continuous HT coupling of the alkylthiophene building blocks. Scheme 16 outlines the synthetic routes developed over recent years for the preparation of regioregular P3ATs (Scheme 16b–f).

3.2.2. Regioregular Poly(3-alkylthiophene)s

In recent years two attractive synthetic routes have emerged for the synthesis of highly regioregular poly(3-alkylthiophene)s P3AT (regioregularity $\geq 98\,\%$) with high molecular weight ($M_n \geq 20000\ g\,mol^{-1}$): the reductive coupling of dibromo monomers with specially activated metals, preferably zinc, according to Rieke and co-workers (Scheme 16e), and the so-called "Grignard metathesis" according to McCullough and co-workers (GRIM) by reaction of dibromo monomers with methyl magnesium bromide and subsequent nickel-catalyzed coupling of the resulting mono-Grignard intermediate (Scheme 16f). The main advantage of both methods compared with the other reactions shown in Scheme 16b–d is the simple preparation of the thiophene monomer 2,5-dibromo-3-alkylthiophene. Compared with the GRIM method, the Rieke reaction has the disadvantage that the regioregularity depends somewhat on the reaction temperature selected. Interestingly, the GRIM method in particular appears to follow a chain-growth mechanism brought about by a preferred transfer of the active metal center to the respective chain end.[54]

The methods listed in Scheme 16b–f provide P3ATs with generally high regioregularities. The extent of regioregularity has a dramatic effect on the morphology and the physical properties of the polymers in the solid state. Charge-carrier mobilities of up to $0.1\ cm^2\,V^{-1}\,s^{-1}$ [55] have been described for the highly regioregular poly(3-hexylthiophene) (P3HT) in OFETs processed from chloroform (for comparison: OFETs prepared from regioirregular PHT show a very low charge-carrier mobility of 10^{-5}–$10^{-4}\ cm^2\,V^{-1}\,s^{-1}$). The charge-carrier mobility of P3HT is highly dependent on the solvent used (differences of up to two orders of magnitude); the best results are obtained with the use of chloroform.[56] It is now considered experimentally confirmed that the regioregular P3ATs are partially crystalline and crystallize in laminar layer domains, in which the layers of "surface-to-surface" stacked polythiophene "main chains" are separated by layers of isolating alkyl side chains. Highly regioregular P3AT thus

usually forms a laminated structure with a vertical arrangement of the thiophene molecular axis relative to the substrate, (the π–π stacking alignment is parallel to the substrate; Figure 14).[57] Kuivalainen and co-workers demonstrated in a

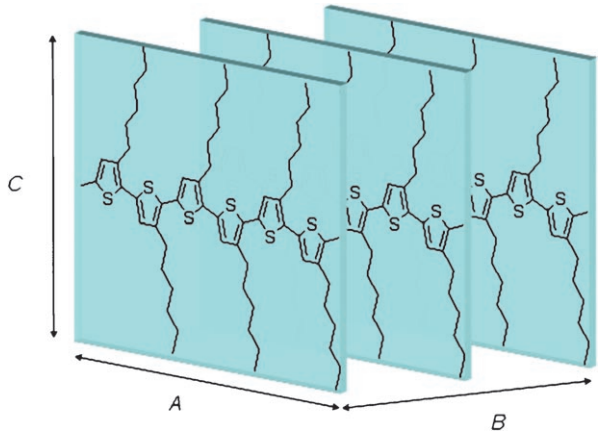

Figure 14. Model for the packing of poly(3-hexylthiophene) (P3HT) in the solid state (*A*: orientation of the molecular axes; *B*: intermolecular stacking direction; *C*: orientation of the alkyl side groups).

Table 2: Molecular masses of the investigated poly(3-hexylthiophene) (P3HT) fractions (from Zen et al.[58]).

Fraction	M_n [g mol^{-1}]	M_w [g mol^{-1}]	PD[a]	DP[b]
1	19000	25650	1.35	114
2	13800	20400	1.48	83
3	5600	6600	1.18	33
4	2200	3100	1.43	13

[a] PD = polydispersity; [b] DP = degree of polymerization (calculated from M_n).

Table 3: OFET charge-carrier mobilities (top gate) in the saturation region and on/off ratios for P3HT fractions 1–4 (immediately after preparation and after tempering at 150 °C for 5 min; from Zen et al.[58]).

Fraction	Charge-carrier mobilities [cm^2 V^{-1} s^{-1}]	on/off ratio
1	2.6×10^{-3}	38000
1, tempered	4.2×10^{-3}	80000
2	1.3×10^{-3}	19000
2, tempered	4.7×10^{-4}	8100
3	1.6×10^{-5}	270
3, tempered	4.3×10^{-5}	1100
4	5.5×10^{-7}	12
4, tempered	2.5×10^{-6}	35

comparative study of poly(3-alkylthiophene)s with alkyl side chains of different length that the charge-carrier mobility μ decreases with increasing length of the alkyl chain from butyl to decyl; this result is attributable to the isolating properties of the alkyl side chain. The OFET charge-carrier mobilities $\mu_{FET,sat}$ of freshly prepared P3AT films (spin coating from chloroform) fall from 2×10^{-4} cm^2 V^{-1} s^{-1} for poly(3-butylthiophene) to $\mu_{FET,sat}=6\times10^{-7}$ cm^2 V^{-1} s^{-1} for poly(3-decylthiophene).[58] Nevertheless, the absolutely highest charge-carrier mobilities were measured for thermally posttreated poly(3-hexylthiophene) (up to 0.1 cm^2 V^{-1} s^{-1}). Owing to its high glass-transition temperature, poly(3-butylthiophene) is largely resistant to thermal posttreatment. The best compromise between optimized solubility and processability (longest possible alkyl side chain) and maximum charge-carrier mobility (thinnest possible layer of isolating alkyl lamella in the solid state) is reported for a side-chain length of six carbon atoms in P3HT.

Zen et al. investigated the influence of the molecular weight of P3HT on the OFET charge-carrier mobility.[59] On the basis of different polymer fractions, a dramatic increase in charge-carrier mobility with increasing P3HT molecular weight was established (M_n = 2200–19000 g mol^{-1}; charge-carrier mobilities increase from 5.5×10^{-7} for the low molecular weight P3HT fraction 4 to 2.6×10^{-3} cm^2 V^{-1} s^{-1} for the high molecular weight P3HT fraction 1; Tables 2 and 3).

Similar observations were also published around the same time by McGehee and co-workers.[60] Both groups reported that the layers of low molecular weight P3HT at first appear more crystalline; individual, extended crystallites can be unambiguously identified in AFM measurements of the thin films. Moreover, diffraction experiments show a very high order in the chains within these crystallites. In contrast, the films of high molecular weight polymers appear less ordered; individual crystallites could not be identified. McGehee and co-workers concluded from this observation that the low charge-carrier mobility in the low molecular weight fractions is attributable to charge-carrier traps at the crystal boundaries of the crystallites, whereas high charge-carrier mobilities ought to be present throughout in the highly ordered crystalline domains. This finding was also supported by the investigations of Sirringhaus and co-workers.[61] Neher and co-workers argued that the charge-carrier mobility depends on the mean crystallinity of the P3HT and not on the perfect packing of individual crystallites.[62] On the basis of deuterated P3HT samples, they found that the P3HT crystallites were generally embedded in an amorphous matrix. Both views do not contradict one another and describe partial aspects of the observed effects.

In high molecular weight P3HT, the ordered regions should be actively connected electronically through the presence of long polymer chains, whereas these electronic connections are absent in the low molecular weight P3HT. Electronic isolation of the crystallites would thus be the reason for the significant drop of the charge-carrier mobility in low molecular weight P3HT. A readily visible indicator for the increasing mean order of P3HT films with increasing molecular weight is a deepening in the color of the films from orange to violet as seen in Figure 15.

p-Semiconductor materials with low ionization potential (typically smaller than 4.9–5.0 eV), for example, also regioregular P3HT, are sensitive to oxidation and tend towards unwanted shifts of the threshold voltage U_T on storage or during operation of the OFET devices. This behavior was attributed to the primary formation of loose, reversible

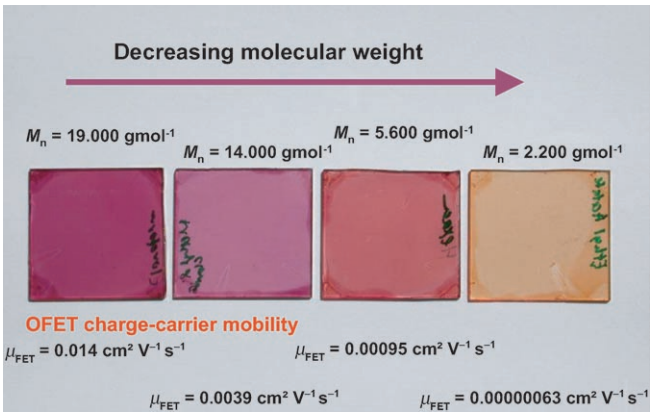

Figure 15. Photographs of thin P3HT films with different molecular weights (for the molecular weights of the fractions see Table 2).

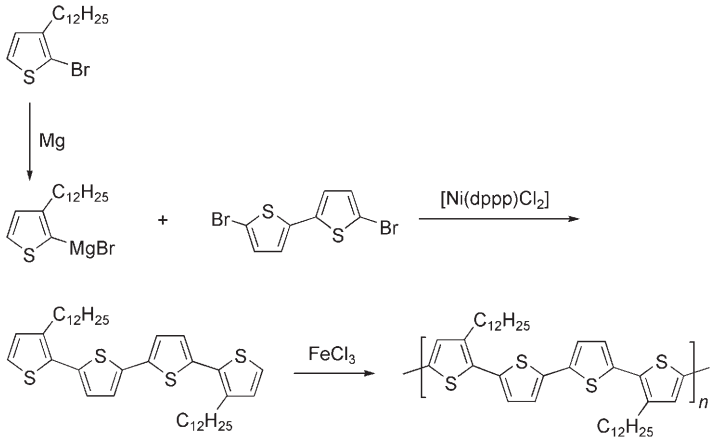

Scheme 17. Synthesis of poly(3,3‴-bisdodecylquaterthiophene) (PQT).

"charge-transfer" (CT) complexes with oxygen (doping). Ficker et al. were indeed able to document that P3HT has a very low photooxidative stability.[63] They exposed non-encapsulated transistor components with P3HT as semiconductor to UV light in the presence of oxygen. At the same time they were also able to detect the irreversible formation of carbonyl defect sites in the polymer backbone by IR spectroscopy. These defects arise in a reaction sequence with a Diels–Alder reaction of singlet oxygen with the diene system of the thiophene ring as initial step. A disruption of conjugation, the formation of trap states for charge carriers, and thus a reduction in charge-carrier mobility is associated with the formation of such defect sites.

The stability towards oxidation of polythiophenes can be improved by an increase in the ionization potential, for example, by a distortion of the coplanar main-chain conformation (change in the substitution pattern of the side chain) or through the incorporation of nonconjugated comonomer building blocks into the main chain.[64] With a small fraction of nonplanar or nonconjugated comonomer building blocks, the resulting materials still form lamellar solid-state structures with P3HT-like field-effect mobilities with significantly increased storage and operating stability.

3.2.3. *Poly(quaterthiophene)s*

In 2004, Ong et al. published a derived class of solution-processable, regioregular polythiophenes, so-called poly(3,3‴-dialkylquaterthiophene)s (PQTs), which have excellent OFET properties.[65]. Their processing can be carried out under ambient conditions (no exclusion of light, oxygen, or humidity), which is attributed to a slightly increased ionization potential (difference to P3HT 0.1–0.2 eV). The PQTs contain longer alkyl side chains (C_{12}), but only on every second thiophene ring. In the synthesis, the monomer 3,3‴-dialkylquaterthiophene is coupled oxidatively with $FeCl_3$ (Scheme 17).

The separation of conjugated main chain and alkyl side chains leads as with P3HT to the formation of three-dimensional, lamellar solid-state structures. The resulting OFET mobilities $\mu_{FET,sat}$ were found to be 0.02–0.05 cm^2 V^{-1} s^{-1} (on/off ratio ca. 10^6). After tempering of the PQTs at 120–140 °C, the OFET charge-carrier mobility $\mu_{FET,sat}$ remained almost unchanged at 0.014 cm^2 V^{-1} s^{-1} (on/off ratio 10^7). A transistor prepared from PQT nanoparticles showed a somewhat increased charge-carrier mobility of 0.06 cm^2 V^{-1} s^{-1} after tempering. OFET components prepared from PQT semiconductors show a high storage stability: the OFET characteristics change only insignificantly when the components were stored under ambient conditions for a month in the dark.

A year later Ong and co-workers also reported the synthesis of poly(3,3″-dialkylterthiophene)s (PTT) (Figure 16) and their use as semiconductors in OFETs.[66] The monomer 3,3″-dialkylterthiophene was prepared by a Suzuki coupling and likewise coupled oxidatively with $FeCl_3$.

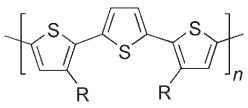

R = *n*-$C_{10}H_{21}$

PTT

Figure 16. Structure of poly(3,3″-dialkylterthiophene) (PTT).

The molecular weights (M_n) are around 16000 g mol^{-1}. X-ray diffractometric investigations on films processed from chloroform show a slight twisting of the thienyl building blocks along the main chain. In this way, the packing density in the lamellar PTT layers falls, but the ionization potential increases slightly. The OFET charge-carrier mobilities measured are in the region of 0.015–0.022 cm^2 V^{-1} s^{-1} at an on/off ratio of 10^5–10^6. Stability investigations after storage for 30 days under atmospheric conditions revealed only a slightly reduced on/off ratio (10^5). In contrast, P3HT shows a large decrease in the on/off ratio of 10^5 to 10^2 under comparable conditions.[67] In 2005, McCulloch et al. also synthesized unsymmetrically substituted terthiophenes (Figure 17) and used them as semiconductors in OFETs.[68] These products again show an increased stability towards oxidation relative to P3HT, but only low charge-carrier mobilities of 10^{-4}–

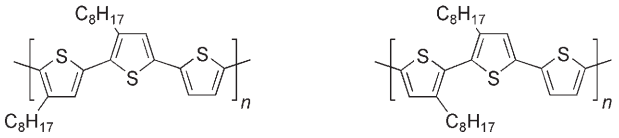

Figure 17. Structures of unsymmetrically substituted poly(terthiophene)s.

10^{-5} $cm^2V^{-1}s^{-1}$ (on/off ratio 10^3), and are thus unsuitable for use as polymeric semiconductors in organic field-effect transistors.

In 2006, McCulloch et al. reported on poly[2,5-bis(3-alkylthiophen-2-yl)thieno[3,2-*b*]thiophene]s (PBTTT) as a new class of polymeric semiconductor materials for OFET devices with alkyl substituents R = $C_{10}H_{21}$, $C_{12}H_{26}$, and $C_{14}H_{29}$ (Figure 18).[69] The dibromothieno[3,2-*b*]thiophene monomers were treated with corresponding distannylated 4,4′-dialkylbithiophene comonomers in a Stille cross-coupling reaction. The number average molecular weights (M_n) were around 30000 g mol^{-1}.

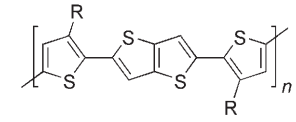

R = *n*-$C_{10}H_{21}$, *n*-$C_{12}H_{25}$, *n*-$C_{14}H_{29}$

PBTTT

Figure 18. Structure of poly[2,5-bis(3-alkylthiophene-2-yl)thieno[3,2-*b*]thiophene] (PBTTT).

Very high maximum charge-carrier mobilities $\mu_{FET,sat}$ were achieved in top-gate OFETs (channel length: 20 μm; channel width: 10 mm): They were around 0.6 $cm^2V^{-1}s^{-1}$ (R = $C_{14}H_{25}$; on/off ratio > 10^7) if the gate insulator (thermal SiO_2) was silanized. Without this treatment step, charge-carrier mobilities of only around 5×10^{-3} $cm^2V^{-1}s^{-1}$ were measured with the same OFET construction. Stability investigations under ambient conditions (4 % relative humidity) showed a charge-carrier mobility of a notable 0.15 $cm^2V^{-1}s^{-1}$ with an on/off ratio of 8×10^7 after storage for 20 days.

Recently, Ong and co-workers also reported a poly[4,8-dihexyl-2,6-bis(3-hexylthiophen-2-yl)benzo[1,2-*b*:4,5-*b*′]dithiophene] (Figure 19).[70] The number average molecular weights (M_n) achieved were around 16300 g mol^{-1}. The polymer with condensed benzodithiophene building blocks showed a very high charge-carrier mobility $\mu_{FET,sat}$ of 0.15–0.25 $cm^2V^{-1}s^{-1}$ (on/off ratio 10^5–10^6) in the top-gate OFETs investigated, which was achieved without thermal posttreatment (!). Long-term storage investigations carried out over

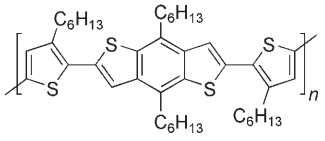

Figure 19. Structure of poly[4,8-dihexyl-2,6-bis(3-hexylthiophene-2-yl)benzo[1,2-*b*:4,5-*b*′]bithiophene].

30 days showed no significant changes in the transistor characteristics. This conjugated polymer is thus a very promising candidate for a roll-to-roll mass production process of TFT-based circuits.

3.2.4. *Polyfluorenes and Fluorene-Type Copolymers*

Fluorene-based homo- and copolymers have been long considered very attractive blue-emitter materials for organic light-emitting diodes (OLEDs). The OLED devices are characterized, among others, by a low operating voltage and high OLED efficiency. Room-temperature TOF measurements on poly(9,9-dioctylfluorene) (PFO) films with a film thickness of 2–3 μm show a maximum hole mobility μ_{TOF} 10^{-3} $cm^2V^{-1}s^{-1}$ if the nematic liquid-crystalline PFO was oriented on a rubbed polyimide layer, relative to a charge-carrier mobility of only 10^{-4} $cm^2V^{-1}s^{-1}$ for the isotropic polymer film.[71] Babel and Jenekhe reported on OFETs from binary blends of regioregular P3HT and poly(9,9-dioctylfluorene) (PFO) in different mixture ratios.[72] AFM images of the blends show spherical clusters, which suggests a phase-separated system. The transistors prepared from it proved to be stable in air and showed p-semiconductor behavior. Charge-carrier mobilities of 2×10^{-4}–1×10^{-3} $cm^2V^{-1}s^{-1}$ depending on the P3HT/PFO mixture ratio were determined, with a maximum on/off ratio of 700.

OFETs with oligofluorenes as semiconductor layers have been described by Tsutsui, Chen, and co-workers.[73] They investigated hepta- and dodecafluorenes with different branched alkyl side chains in the 9,9-position of the fluorene unit (Figure 20) in a top-gate configuration and compared the

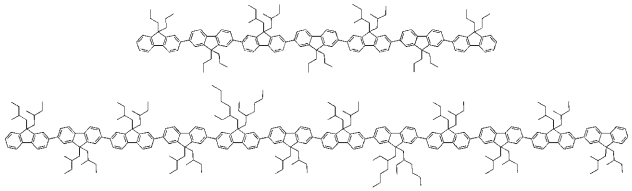

Figure 20. Structures of the investigated hepta- and dodecafluorenes.

data with poly(9,9-dioctylfluorene) (PFO) as polymeric semiconductor. The OFETs were constructed on rubbed and non-rubbed polyimide layers and the films of oligomers and polymers were spin coated from chloroform. The rubbed polyimide substrate was then used for the preparation of oriented semiconductor layers of the throughout nematic liquid-crystalline oligo- and polyfluorenes. The hole mobilities $\mu_{FET,sat}$ achieved increased for the fluorene dodecamer on transition from the amorphous to the glassy nematic phase from 1×10^{-5} $cm^2V^{-1}s^{-1}$ by about 800 fold to 1.2×10^{-3} $cm^2V^{-1}s^{-1}$ at a maximum on/off ratio of 10^4.

The charge-carrier mobility of the poly(9,9-dialkylfluorene)s is limited by the out-of-plane configuration of the side chains, since the polymers in the solid state can only form two-dimensional lamellar structures to a limited extent (the so-called β phase of PFO). In this way, the intermolecular transport of the charge carriers is impeded, which limits the

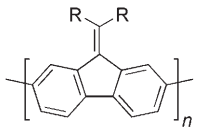

R = $C_{10}H_{21}$, $C_{12}H_{25}$, $C_{14}H_{29}$

Figure 21. Structure of poly(alkylidenefluorene).

charge-carrier mobility. To circumvent this restriction, poly(alkylidenefluorene)s with in-plane alkyl substituents were prepared and characterized by Heeney et al. (Figure 21).[74]

These products have an sp^2-hybridized carbon atom in the 9-position, and the alkyl side chains of the alkylidene groups are thus aligned coplanar (in-plane) to the polymer backbone. In this way, a cofacial aggregation is made simpler, which leads to reduced intermolecular distances (< 4 Å) of the polymer chains. The molecular weights (M_n) of the polymers obtained were 4000 to 14000 g mol^{-1}. In OFETs, charge-carrier mobilities of up to 3×10^{-3} cm^2 V^{-1} s^{-1} at an on/off ratio of 10^6 were measured. Tempering of the transistors to 170 °C (30 min)—somewhat above the glass-transition temperature of the polymers (ca. 150 °C)—produced no significant improvement in the charge-carrier mobility.[75]

3.2.5. *Alternating Thiophene-Based Copolymers*

Alternating 9,9-dioctylfluorene/bithiophene copolymers (F8T2) were first used in OFETS by Sirringhaus et al. F8T2 forms a thermotropic nematic LC phase above 265 °C and can be oriented on a rubbed polyimide layer. In the synthesis of F8T2, 2,7-bis(1,3,2-dioxaborolan-2-yl)-9,9-di-*n*-octylfluorene is treated with 5,5′-dibromo-2,2′-bithiophene in a Suzuki aryl–aryl cross-coupling reaction (Scheme 18).[76]

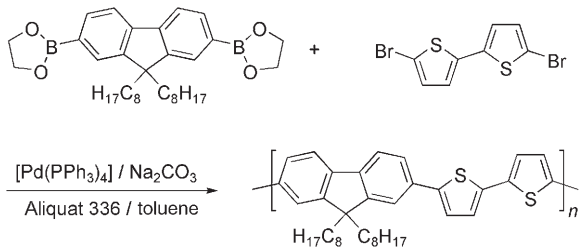

Scheme 18. Preparation of alternating 9,9-dioctylfluorene/bithiophene copolymers (F8T2).

The number average molecular weights (M_n) of the F8T2 obtained were around 60000 g mol^{-1}. In the preparation of the transistors, a polyimide layer is first applied to a suitable substrate, which is then mechanically rubbed. The gold source and drain electrodes are then attached photolithographically. The F8T2 polymer film is then applied by spin coating from xylene. The F8T2 chains are then aligned parallel to the direction of rubbng by tempering for 15 minutes in the LC phase at 285 °C. In the top-gate configuration, the oriented F8T2 layer obtained shows a maximum charge-carrier mobility $\mu_{FET,sat}$ of 0.009–0.02 cm^2 V^{-1} s^{-1} with parallel alignment of the polymer chains relative to the comb electrode. The threshold voltages are at 1–10 V very small and, in comparison with those of P3HT, essentially independent of the gate voltage.[77] In 2001, Sirringhaus et al. reported an all-polymer transistor prepared by inkjet printing with F8T2 as semiconductor material.[78] In this case, the source and drain electrodes of PEDOT/PSS were first printed onto a polyimide-coated substrate. The semiconductor was then spin coated and aligned by high-temperature treatment. Insulator poly(vinylphenol) (PVP) was then printed and finally the gate electrodes, also of PEDOT/PSS, were applied by inkjet printing. The top-gate transistors thus obtained had charge-carrier mobilities in the saturated region of 0.02 cm^2 V^{-1} s^{-1} with an on/off ratio of 10^5.

An alternative approach for the application of the polymeric semiconductor F8T2 by means of the so-called "friction-transfer" technique was described by the company Epson.[79] The polymer material to be applied is molded into a block, which is drawn over a hot substrate under pressure to generate the (oriented) material. The advantage of this method is film preparation without solvents. With this method, F8T2 is deposited at 230 °C in the form of oriented "nanowires". A top-gate transistor prepared by this method with gold electrodes, a 400-nm-thick F8T2 layer, a 1500-nm-thick layer of an unspecified insulator, and a spin-coated PEDOT/PSS gate electrode showed a charge-carrier mobility $\mu_{FET,sat}$ of 3.5×10^{-3} cm^2 V^{-1} s^{-1} (on/off ratio of 10^6) when the "nanowires" are aligned parallel to the source–drain channel.

Shim and co-workers attempted to improve the transistor characteristics of such copolymers by incorporating condensed cyclic compounds such as pentacene, benzodithiophene, thienothiophene, and dithienothiophene into the polymer chain.[80] Alternating fluorene/thieno[3,2-*b*]thiophene copolymers (F8TT; Figure 22) show maximum OFET charge-carrier mobilities of 1.1×10^{-3} cm^2 V^{-1} s^{-1}. The com-

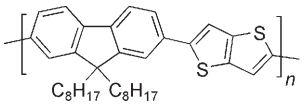

F8TT

Figure 22. Structure of poly[9,9-dioctylfluorene-*alt*-thieno[3,2-*b*]thiophene] (F8TT).

parable transistor with F8T2 as semiconductor under similar conditions gave a mobility $\mu_{FET,sat}$ of 0.4×10^{-3} cm^2 V^{-1} s^{-1}. Shim and co-workers attributed the increased mobility to a higher ordered F8TT solid-state structure. However, by tempering the transistor at 285 °C, the charge-carrier mobility for F8TT dropped to 10^{-5} cm^2 V^{-1} s^{-1}, which was explained by a partial recrystallisation of the F8TT film and the resulting formation of charge-carrier traps at the crystal boundaries.

In 2002, Asawapirom et al. published a series of alternating copolymers of fluorene and oligothiophene building blocks as possible OFET semiconductor materials. These were prepared in a Stille coupling from 9,9-dialkylated dibromofluorene and bisstannylated oligothiophenes (molecular weight (M_n) up to 19000 g mol^{-1}; Figure 23). A few of the fluorene/oligothiophene copolymers form stable, nematic LC phases between 219 and 233 °C,; the maximum charge-carrier mobilities $\mu_{FET,sat}$ were 1.1×10^{-3} cm^2 V^{-1} s^{-1}.[81] Müllen and co-

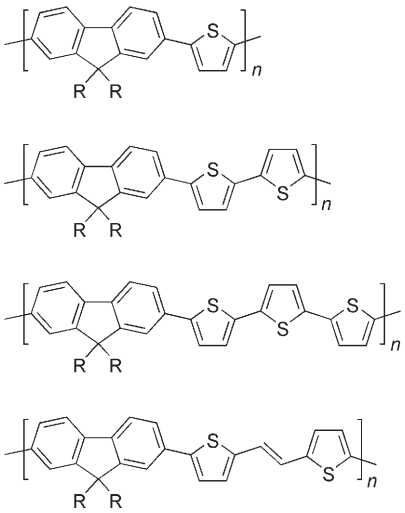

Figure 23. Alternating fluorene/oligothiophene copolymers.

workers recently reported on the use of alternating benzothiadiazole/cyclopentadithiophene copolymers (Figure 24) as semiconductor layer in bottom-gate/bottom-contact OFETs.[82a] After tempering of the drop-coated substrates (solvent 1,2,4-trichlorobenzene; substrate temperature: 100 °C) at 200 °C for 2 hours, unusually high hole mobilities $\mu_{FET,sat}$ of up to 0.17 $cm^2V^{-1}s^{-1}$ were observed.

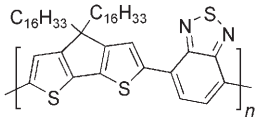

Figure 24. Structure of an alternating benzothiadiazole/cyclopentadithiophene copolymer.

The insertion of the benzothiadiazole acceptor units should greatly increase the storage stability. Similar copolymers with modified alkyl side groups (ethylhexyl in place of hexadecyl) have been used by Brabec and co-workers in highly efficient organic solar cells of the bulk heterojunction type.[82b]

3.2.6. *Poly(2,5-thienylenevinylene)s*

A further class of polymers that is of interest as semiconductor materials for solution-processed organic transistors are poly(2,5-thienylenevinylene)s (PVTs; Figure 25).

In 1993, Fuchigami et al. were the first to describe the use of unsubstituted PTV in OFETs. Since PTV is insoluble in organic solvents, a soluble precursor polymer—poly[2,5-thienylene(1′-methoxy)ethylene]—was synthesized by the method of Saito and Murase, which after film formation (spin coating) onto a chromium gate electrode was converted into the semiconducting PTV by loss of methanol by heating to 200 °C (5 min with nitrogen/HCl gas).[83] Very high charge-carrier mobilities $\mu_{FET,sat}$ of up to 0.22 $cm^2V^{-1}s^{-1}$ were measured in bottom-gate transistors with PTV as active layer.[84] Integrated circuits with all-polymer construction and PTV as active semiconductor layer were described by Philips in 1998. The electrodes of the top-gate transistors investigated were prepared from doped polyaniline, a dielectric of polyvinylpyrrolidone was spin coated between the semiconductor layer and the gate electrode. The OFET mobilities $\mu_{FET,sat}$ achieved were around 3×10^{-4} $cm^2V^{-1}s^{-1}$ for a channel width of 1 mm and a channel length of 2 μm.[85]

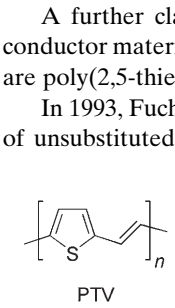

PTV

Figure 25. Structure of poly(thienylenevinylene) (PTV).

The highly promising OFET results prompted an intensive search for the simplest possible synthetic route for PTV with high molecular weight. The previously used precursor polymers for poly(thienylenevinylene) were prepared from disulfonium monomers by the Wessling–Zimmerman route from dihalo monomers by the dehalogenation route according to Gilch et al., or the xanthate/sulfinyl route according to Vanderzande and co-workers, which had all been developed for the preparation of poly(phenylenevinylene)s (PPVs) (Scheme 19).[86] The routes differ in the choice of leaving group (L), the polarizing group (P), and the polymerization conditions. In 2004, Vanderzande and co-workers published a new synthetic route specially developed for PTV via a dithiocarbamate-substituted precursor polymer (Scheme 20). PTV is accessible by this route in high yields with a high weight-average molecular mass M_w of up to 94 000 g mol^{-1} and low defect concentration.

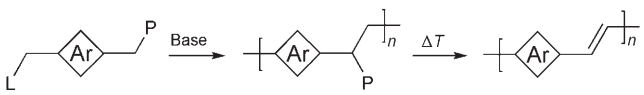

Scheme 19. Precursor pathways to poly(arylenevinylene)s: Wessling–Zimmerman: L = P = SR_2; Gilch: L = P = Cl; xanthate: L = P = SC(S)OR; sulfinyl: L = Cl, P = S(O)R (L = leaving group, P = polarizing group).

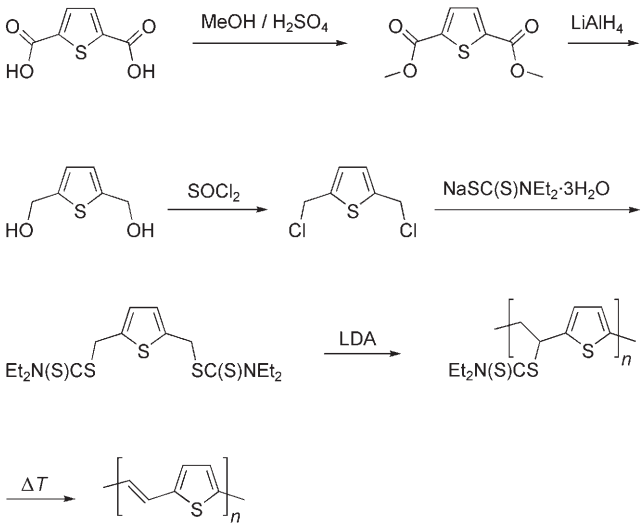

Scheme 20. Preparation of PTV by the dithiocarbamate route.

The soluble precursor polymer is generated by the reaction of the dithiocarbamate monomers with lithium diisopropylamide (LDA) in the initiating deprotonation step. The polymer-analogous conversion into PTV takes place by slow heating of the initially formed saturated precursor polymers in the solid state to up to 350 °C with a heating rate of 2 K min^{-1}. The transistor properties were tested in a top-gate OFET with PTV as active semiconductor layer (channel length: 75 μm; channel width: 2 mm). Source and drain electrodes were of gold, the gate electrode of aluminum. The whole device was heated slowly to 185 °C for the conversion of the precursor polymer. The charge-carrier mobilities achieved were 1.7×10^{-3} cm^2 V^{-1} s^{-1} at an on/off ratio of approximately 10^4.[87] Still unclear is whether the very low conversion temperature of 185 °C is sufficient for a complete formation of the conjugated system.

In 2005, TNO Industrial Technology described a soluble PTV that contained a solubilizing side chain on the thiophene ring ($M_n = 26000$ g mol^{-1}). However, only a low hole mobility $\mu_{FET,sat}$ of 10^{-3} cm^2 V^{-1} s^{-1} was found in OFET devices, which was attributed to the presence of charge-carrier traps.[88]

3.2.7. Polytriphenylamines

In addition to sulfur-containing polythiophenes and corresponding copolymers, nitrogen-containing aromatic polymers—so-called polytriarylamines (PTAAs)—have aroused interest for OFET applications in recent years. The background to this interest is in particular the completely amorphous solid-state structure of the PTAAs, which promises a simple and reproducible processing to thin films or layers.

Low molecular weight or oligomeric triarylamines have long been known as hole conductor materials for the active layer of photocopiers, OLEDs, and organic solar cells. In addition to their advantageous properties such as adequately high charge-carrier mobilities and stability towards air and humidity, the PTAAs and the corresponding oligomers show very good solubility in common organic solvents. In spite of their somewhat lower charge-carrier mobilities $\mu_{FET,sat}$ of 10^{-3}–10^{-4} cm^2 V^{-1} s^{-1} relative to P3HT, PTAAs are highly promising candidates for solution-processable OFETs.[89]

The first preparation of triarylamine dimers and oligomers was carried out by electrochemical oxidation of corresponding triarylamine monomers.[90] In 2000, an electrochemical preparation of polytriarylamines from triphenylamine in an acetonitrile/toluene mixture and Bu_4NPF_6 as electrolyte was described by Petr and co-workers. The highly cross-linked structure of the resulting, insoluble polymers was confirmed in FTIR investigations of polymer films deposited on the electrode. In 2003, Lambert and Nöll reported the electrochemical synthesis of a linear polymer starting from a monomer of two triphenylamine units connected through an acetylene or diacetylene bridge (Figure 26). The linear construction of the polymers is probably brought about by the higher stability of the intermediate radical cations at the growing chain terminus.[91]

Functionalized triarylamine (TAA) monomers can be prepared by palladium-catalyzed amination of aryl halides.

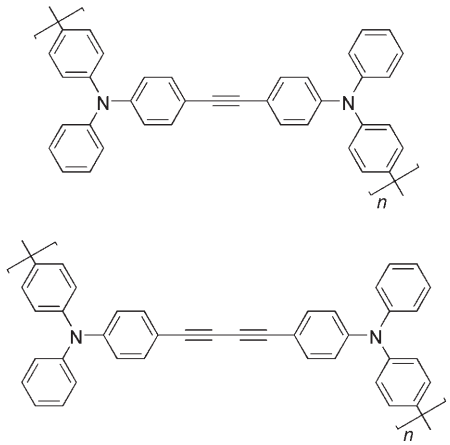

Figure 26. Poly(triarylamine)s with acetylene and diacetylene bridges.

The groups of Buchwald and Hartwig independently developed a method for the efficient preparation of tertiary aromatic amines from primary or secondary amines and aryl halides (Scheme 21).[92] The reaction takes place in the

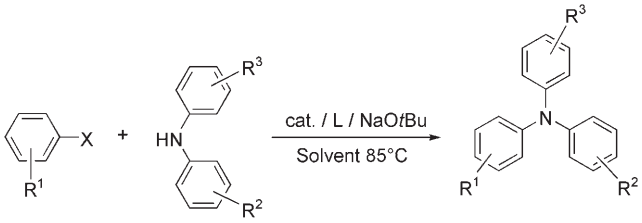

cat. = $[Pd_2(dba)_3]$, $[Pd(dba)_2]$, $Pd(OAc)_2$
L = (+/–)-Binap, dppf, P(*t*Bu)$_3$, P(*o*-Tolyl)$_3$
Solvent = benzene, toluene, xylene

Scheme 21. Synthesis of triarylamine monomers by the Buchwald–Hartwig coupling method. R^1–R^3 = H, alkyl; Binap = 2,2′-bis(diphenylphospanyl)-1,1′-binapthyl; dba = *trans*,*trans*-dibenzylideneacetone.

presence of a palladium catalyst (e.g. $[Pd_2(dba)_3]$, $[Pd(dba)_2]$ or $Pd(OAc)_2$), combined with phosphine ligands (e.g. (+/−)-Binap, dppf, P(*o*-tolyl)$_3$, or P(*t*Bu)$_3$) in aromatic solvents such as benzene, toluene, or xylene under strongly alkaline conditions. Several problems arose in the direct transfer of this C–N coupling method for the preparation of polymers (PTAAs) using difunctional monomers, such as the incorporation of phosphorus atoms from the phosphine ligands into the main chain, or the formation of cyclic oligomers. In 1999, Hartwig and co-workers overcame these problems with tailor-made phosphine ligands and by the use of functional oligomers as starting components.[93]

In 2002, Veres et al. reported for the first time PTAAs as solution-processable, organic materials for OFETs.[94] They used as polymer formation reaction a reductive aryl–aryl coupling of dihalotriarylamine monomers by the method of Yamamoto. The synthesis of the dihalo monomers was carried out by the coupling of 1-chloro-4-iodobenzene with substituted aniline derivatives in a Ullmann reaction, exploiting the

chloro–iodo selectivity. The poly(triphenylamine)s (PTPAs) as target molecules were then prepared by a metal-catalyzed aryl–aryl homocoupling of the dichloro monomers in the presence of nickel chloride/zinc. (Scheme 22).

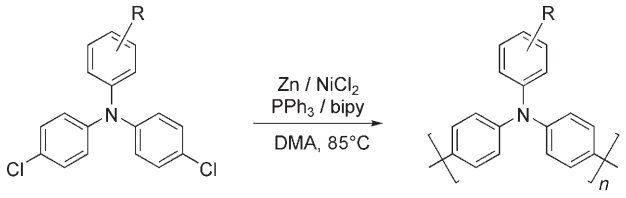

Scheme 22. Synthesis of poly(triphenylamine)s (PTPA). R = H, alkyl.

The number average molecular weight (M_n) of the PTPAs was of the order of 3000 g mol^{-1} with a polydispersity (PD) of 1.5 to 1.9. Monofunctional *p*-chlorotoluene was added as end-capping reagent to avoid terminal chlorine substituents. TOF investigations of the polymers showed hole mobilities $\mu_{FET,sat}$ of around 10^{-2} cm^2 V^{-1} s^{-1}. When these polymers were used as active semiconductor layers in OFET devices in bottom-gate geometry, charge-carrier mobilities $\mu_{FET,sat}$ of 2×10^{-3} cm^2 V^{-1} s^{-1} with an on/off ratio of 2.3×10^5 were measured.

In the following years, Veres and co-workers concentrated on the optimization of the OFET devices.[95] It was established that the construction of the transistor (top gate or bottom gate), the gate insulator, and the structure of the semiconductor–insulator interface play a pivotal role for the device characteristics. In the bottom-gate configuration, it was demonstrated that the resulting morphology of the semiconductor material at the interface is greatly influenced by the dielectric. An increased interface roughness can lead to morphological and topological trap states that function as charge-carrier traps and lower the charge-carrier mobility. Surface treatment of the dielectric is beneficial, but not readily possible with devices in the top-gate configuration. Consequently organic dielectrics such as PMMA or PVP are preferred. The use of polymer gate insulators with very low dielectric constants allows a further increase in charge-carrier mobility. Maximum charge-carrier mobilities with PTPA as semiconductor of around 5×10^{-3} cm^2 V^{-1} s^{-1} in top-gate OFETs were achieved with nonpolar resins such as CYTOP as gate insulator instead of the originally used PMMA and PVP layers (Table 4).

In 2005, Hübler and co-workers published the first printed organic field-effect transistors based on PTPA materials.[96] A PTPA (PTPA3, Figure 27) with significantly improved solubility and higher molecular weight was also used. The increase in solubility was achieved by increasing the substitution density of methyl groups on the non-chain-forming phenyl ring. The OFETs showed a charge-carrier mobility $\mu_{FET,sat}$ of 3×10^{-3} cm^2 V^{-1} s^{-1} (on/off ratio 2×10^5). An investigation of the stability towards oxidation of PTPA-based printed OFET devices showed a significantly increased storage and air stability relative to fluorene/bithiophene copolymer (F8T2)-based transistors. The PTPA-based OFETs could be stored for a year in air without the OFET properties being dramatically changed. The PTPA-based devices showed only a slightly lowered charge-carrier mobility (before: 3×10^{-3} cm^2 V^{-1} s^{-1}; after: 1.3×10^{-3} cm^2 V^{-1} s^{-1}). In comparison, transistors with F8T2 as active layer (initial charge-carrier mobility: $\mu_{FET,sat}=2\times10^{-3}$ cm^2 V^{-1} s^{-1}) showed no OFET behavior after storage for around 2000 hours. UV irradiation of the F8T2-based OFETs for 15 minutes also caused a complete loss of the transistor properties of the semiconductor, whereas the charge-carrier mobility of PTPA-based transistors differed by only about 20% after UV irradiation for 60 minutes. However, with longer irradiation the charge-carrier mobilities dropped significantly, which suggests a degradation of the polymeric semiconductor layer.

In 2005, Ong and co-workers introduced polyindolo[3,2-*b*]carbazoles (Figure 28) as new p-semiconductor polymers for solution-processed OFETs ($M_n=11\,200$ g mol^{-1}). After optimization of the side chain R and the dielectric, a maximum hole mobility $\mu_{FET,sat}$ of 2×10^{-2} cm^2 V^{-1} s^{-1} in bottom-gate OFETs was achieved with R = *n*-octyl and polystyrene as dielectric.[97]

Table 4: Maximum OFET charge-carrier mobilities for poly(triphenylamine) semiconductors with different gate isolators in different OFET geometries (from Veres et al.[94]).

Gate isolator	k[a]	PTPA	Transistor geometry	μ_{FET} [cm^2 V^{-1} s^{-1}]
CYTOP	2.1	PTPA2	top gate	5×10^{-3}
CYTOP	2.1	PTPA2	top gate	2×10^{-3}
poly(propylene-*co*-butene)	2.3	PTPA1	top gate	2.6×10^{-3}
poly(propylene-*co*-butene)	2.3	PTPA1	bottom gate	2×10^{-3}
PVP	4.5	PTPA1	top gate	5.2×10^{-4}
PMMA	3.5	PTPA1	top gate	4.9×10^{-4}
PMMA	3.5	PTPA2	top gate	5.5×10^{-4}
PVP-*co*-PMMA	3.5–4	PTPA1	top gate	4.6×10^{-4}

[a] Dielectric constant of the gate isolator.

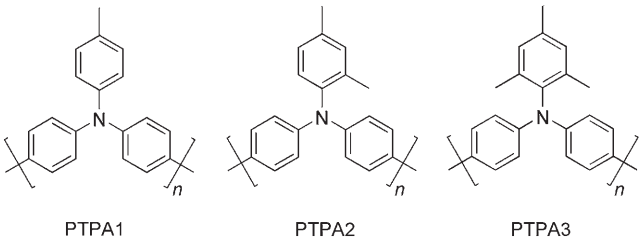

Figure 27. Structure of poly(triphenylamine) (PTPA) with different substitution patterns on the side-chain phenyl substituents.

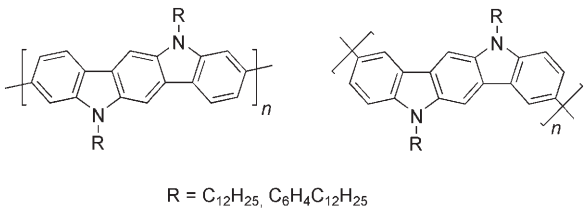

Figure 28. Structure of poly(indolocarbazol)s.

4. Summary and Outlook

The present review attempts to give an overview of new semiconductor materials for solution-processed, organic field-effect transistors from the viewpoint of synthetic chemistry. The use of solution-processing techniques, such as spin coating, screen printing, and inkjet printing, or conventional printing methods for the production of electronic devices promises the development of new applications such as "cost-effective mass production" (roll-to-roll) or "large-area, electronic circuits on flexible substrates". Soluble organic semiconductors (both low molecular mass and oligomeric materials as well as polymeric materials) have decisive advantages for these applications.

The strictly applied clear distinction of a few years ago between polymers and "small molecules" has today almost completely vanished; pivotal is the ability of materials to be processed from solution into topologically and morphologically homogeneous films. This includes in the first instance adequate solubility of the materials in organic solvents. Strategies for increasing the solubility, such as the so-called precursor routes using soluble precursors of the actual insoluble materials, or the introduction of solubilizing substituents, have been extensively explored. Care must be taken when introducing solubilizing side chains that these substituents do not signicantly disrupt the formation of an ordered solid-state structure with optimal intermolecular interactions, since these interactions are critical for charge-carrier transport in electronic devices. Secondly, optimal film formation properties are pivotal. Whereas this usually does not represent a problem with amorphous, glassy materials, crystalline compounds must also be processable to homogeneous micro- or nanocrystalline layers of low roughness. Of advantage here is often the additional possibility to be able to achieve a further increase in the structural long-range order in a subsequent thermal postprocessing step.

In this exciting field, numerous solution-processable semiconductor materials for organic field-effect transistors have been developed in recent years which show highly promising electronic properties in the active semiconductor layers prepared from them, such as high charge-carrier mobilities of up to 1 $cm^2 V^{-1} s^{-1}$, high on/off ratios greater than 10^5, and an impressive stability of the electronic devices under atmospheric conditions. The next two or three years will show whether mature electronic circuits based on solution-processed OFETs will gain entry into the first marketable products. Possible applications include a new generation of electronic article identification devices (so-called RFID tags) for logistic and safety applications, and flexible active-matrix displays with OFET-based control electronics for electronic books, promotional applications, etc. A number of companies worldwide have intensively embraced this development work.

Our own work was supported financially by the Deutsche Forschungsgemeinschaft (SPP 1121 "Organische Feldeffekttransistoren: Strukturelle und Dynamische Eigenschaften") and the BMBF (Förderschwerpunkt Polymerelektronik). H.T. acknowledges the support of the research at Evonik-Degussa by the state of North-Rhien-Westphalia and the European Union. We thank Prof. Dieter Neher and his colleagues at the Universität Potsdam for continuous support and advice. We would like to thank the Institut für Print- und Medientechnik der TU Chemnitz for the friendly supply of the pictorial matter for the frontispiece.

Received: May 2, 2007
Published online: March 20, 2008

[1] a) M. Madru, G. Guillaud, M. Al Sadoun, M. Maitrot, C. Clarisse, M. Le Contellec, J.-J. André, J. Simon, *Chem. Phys. Lett.* **1987**, *142*, 103 – 105; b) H. Koezuka, A. Tsumura, T. Ando, *Synth. Met.* **1987**, *18*, 699 – 704; c) C. J. Drury, C. M. J. Mustaers, C. M. Hart, M. Matters, D. M. D. de Leeuw, *Appl. Phys. Lett.* **1998**, *73*, 108 – 110; d) G. H. Gelinck, T. C. T. Geuns, D. M. de Leeuw, *Appl. Phys. Lett.* **2000**, *77*, 1487 – 1489; e) H. E. Katz, Z. Bao, S. L. Gilat, *Acc. Chem. Res.* **2001**, *34*, 359 – 369.

[2] H. Sirringhaus, *Adv. Mater.* **2005**, *17*, 2411 – 2425.

[3] Examples of OFET applications in which the semiconductor has been applied by sublimation: a) C. D. Sheraw, J. A. Nichols, D. J. Gundlach, J. R. Huang, C. C. Kuo, H. Klauk, T. N. Jackson, M. G. Kane, J. Campi, F. P. Cuomo, B. K. Greening, *Tech. Dig. Int. Electron Devices Meet.* **2000**, 619 – 622; b) B. Crone, A. Dodabalapur, Y.-Y. Lin, R. W. Filas, Z. Bao, A. LaDuca, R. Sarpeshkar, H. E. Katz, W. Li, *Nature* **2000**, *403*, 521 – 523; c) C. D. Sheraw, L. Zhou, J. R. Huang, D. J. Gundlach, T. N. Jackson, M. G. Kane, I. G. Hill, M. S. Hammond, J. Campi, B. K. Greening, J. Francl, J. West, *Appl. Phys. Lett.* **2002**, *80*, 1088 – 1090; d) J. A. Rogers, Z. Bao, *J. Polym. Sci. Part A* **2002**, *40*, 3327 – 3334; applications in which the semiconductor was applied from solution: e) H. Sirringhaus, T. Kawase, R. H. Friend, *Mater. Res. Bull.* **2001**, *36*, 539 – 543; f) H. E. A. Huitema, G. H. Gelinck, J. B. P. H. van der Putten, K. E. Kuijk, C. M. Hart, E. Cantatore, P. T. Herwig, A. J. J. M. van Breemen, D. M. de Leeuw, *Nature* **2001**, *414*, 599; g) S. E. Burns, P. Cain, J. Mills, J. Wang, H. Sirringhaus, *Mater. Res. Bull.* **2003**, *28*, 829 – 834; h) Z. Bao, *Nat. Mater.* **2004**, *3*, 137 – 138; i) V. Subramanian, J. M. J. Fréchet, P. C. Chang, D. C. Huang, J. B. Lee, S. E. Molesa, A. R. Murphy, D. R. Redinger, S. K. Volkman, *Proc. IEEE* **2005**, *93*, 1330 – 1338; j) J. Z. Wang, J. Gu, F. Zenhausern, H. Sirringhaus, *Appl. Phys. Lett.* **2006**, *88*, 133502; Single crystal OFETs: A. J. Briseno, R. J. Tseng, M.-M. Ling, E. H. L. Falcao, Y. Yang, F. Wudl, Z. Bao, *Adv. Mater.* **2006**, *18*, 2320 – 2324.

[4] a) G. Horowitz in *Semiconducting Polymers* (Eds.: G. Hadziioannou, P. F. van Hutten), Wiley-VCH, Weinheim, **2000**, p. 463 – 514; b) C. D. Dimitrakopoulos, P. R. L. Malenfant, *Adv. Mater.* **2002**, *14*, 99 – 117; c) J. Veres, S. Ogier, G. Lloyd, D. de Leeuw, *Chem. Mater.* **2004**, *16*, 4543 – 4555; d) Y. Sun, Y. Liu, D. Zhu, *J. Mater. Chem.* **2005**, *15*, 53 – 65; e) A. Facchetti, M.-Y. Yoon, T. J. Marks, *Adv. Mater.* **2005**, *17*, 1705 – 1725.

[5] H. Koezuka, A. Tsumura, T. Ando, *Synth. Met.* **1987**, *18*, 699 – 704.

[6] G. Horowitz, M. E. Hajlaoui, R. Hajlaoui, *J. Appl. Phys.* **2000**, *87*, 4456 – 4463.

[7] a) H. Akimichi, K. Waragai, S. Hotta, H. Sakaki, *Appl. Phys. Lett.* **1991**, *58*, 1500 – 1502; b) S. Hotta, K. Waragai, *J. Mater. Chem.* **1991**, *1*, 835 – 842; c) G. Horowitz, F. Deloffre, F. Garnier, R. Hajlaoui, M. Hmyene, A. Yassar, *Synth. Met.* **1993**, *54*, 435 – 445.

[8] a) T. Weil, U. M. Wiesler, A. Herrmann, R. Bauer, J. Hofkens, F. C. De Schryver, K. Müllen, *J. Am. Chem. Soc.* **2001**, *123*, 8101 – 8108; b) M. Lor et al., *J. Am. Chem. Soc.* **2002**, *124*, 9918 – 9925; c) Y. Shirota, *J. Mater. Chem.* **2005**, *15*, 75 – 93; d) A. Petrella, J. Cremer, L. De Cola, P. Bäuerle, R. M. Williams, *J.*

Phys. Chem. A **2005**, *109*, 11687 – 11695; e) X.-M. Liu, T. Lin, X.-T. Hao, K. S. Ong, C. He, *Macromolecules* **2005**, *38*, 4157 – 4168; f) "cruciform π-conjugated oligomers": F. Galbrecht, T. Bünnagel, A. Bilge, U. Scherf, T. Farell in *Functional Organic Materials* (Eds.: T. Müller, U. H. F. Bunz), Wiley-VCH, Weinheim, **2007**, p. 83 – 118; g) X. Sun, Y. Liu, S. Chen, W. Qiu, G. Yu, Y. Ma, T. Qi, H. Zang, X. Xu, D. Zhu, *Adv. Funct. Mater.* **2006**, *16*, 917 – 925; h) T. P. I. Saragi, R. Pudzich, T. Fuhrmann, J. Salbeck, *Mater. Res. Soc. Symp. Proc.* **2002**, *725*, 85 – 92; i) T. P. I. Saragi, T. Fuhrmann-Lieker, J. Salbeck, *Adv. Funct. Mater.* **2006**, *16*, 966 – 974.

[9] a) M. S. A. Abdou, F. P. Orfino, Y. Son, S. Holdcroft, *J. Am. Chem. Soc.* **1997**, *119*, 4518 – 4524; b) E. J. Meijer, C. Detcheverry, P. J. Baesjou, E. van Veenendaal, D. M. de Leeuw, T. M. Klapwijk, *J. Appl. Phys.* **2003**, *93*, 4831 – 4835; c) B. Ong, Y. Wu, P. Liu, S. Gardner, *J. Am. Chem. Soc.* **2004**, *126*, 3378 – 3379; d) H. Kempa, K. Reuter, M. Bartzsch, U. Hahn, A. C. Huebler, D. Zielke, M. Forster, U. Scherf, *Proc. IEEE Polytronic Conference* **2005**, article no. 1596489, 67 – 71.

[10] H. J. Spencer, P. J. Skabara, M. Giles, I. McCulloch, S. J. Coles, M. B. Hursthouse, *J. Mater. Chem.* **2005**, *15*, 4783 – 4792.

[11] a) V. Podzorov, E. Menard, A. Borissov, V. Kiryukhin, J. A. Rogers, M. E. Gershenson, *Phys. Rev. Lett.* **2004**, *93*, 086602; b) E. Menard, V. Podzorov, S.-H. Hur, A. Gaur, M. E. Gershenson, J. A. Rogers, *Adv. Mater.* **2004**, *16*, 2097; c) T. W. Kelley, D. V. Muyres, P. F. Baude, T. P. Smith, T. D. Jones, *Mater. Res. Soc. Symp. Proc.* **2003**, *771*, 169 – 179.

[12] a) A. R. Brown, A. Pomp, D. M. de Leeuw, D. B. M. Klaasen, E. E. Havinga, P. Herwig, K. Müllen, *J. Appl. Phys.* **1996**, *79*, 2136 – 2137; b) P. T. Herwig, K. Müllen, *Adv. Mater.* **1999**, *11*, 480 – 483.

[13] A. Afzali, C. D. Dimitrakopoulos, T. L. Breen, *J. Am. Chem. Soc.* **2002**, *124*, 8812 – 8813.

[14] S. K. Volkman, S. Molesa, B. Mattis, P. C. Chang, V. Subramanian, *Mater. Res. Soc. Symp. Proc.* **2003**, *769*, 369 – 374.

[15] K. P. Weidkamp, A. Afzali, R. M. Tromp, R. J. Hamers, *J. Am. Chem. Soc.* **2004**, *126*, 12740 – 12741.

[16] A. Afzali, C. D. Dimitrakopoulos, T. O. Graham, *Adv. Mater.* **2003**, *15*, 2066- 2069.

[17] a) J. E. Anthony, J. S. Brooks, D. L. Eaton, S. R. Parkin, *J. Am. Chem. Soc.* **2001**, *123*, 9482 – 9483; b) J. E. Anthony, *Chem. Rev.* **2006**, *106*, 5028 – 5048; synthesis of the alkynyl-substituted pentacenes: c) J. E. Anthony, D. L. Eaton, S. R. Parkin, *Org. Lett.* **2002**, *4*, 15 – 18; d) C. D. Sheraw, T. N. Jackson, D. L. Eaton, J. E. Anthony, *Adv. Mater.* **2003**, *15*, 2009 – 2011; e) C. F. H. Allen, A. Bell, *J. Am. Chem. Soc.* **1942**, *64*, 1253 – 1260.

[18] F. Würthner, R. Schmidt, *ChemPhysChem* **2006**, *7*, 793 – 797.

[19] a) G. Laquindanum, H. E. Katz, A. J. Lovinger, *J. Am. Chem. Soc.* **1998**, *120*, 664 – 672; b) H. E. Katz, W. Li, A. J. Lovinger, J. Laquindanum, *Synth. Met.* **1999**, *102*, 897 – 899.

[20] a) M. M. Payne, S. A. Odom, S. R. Parkin, J. E. Anthony, *Org. Lett.* **2004**, *6*, 3325 – 3328; b) M. M. Payne, S. R. Parkin, J. E. Anthony, C.-C. Kuo, T. N. Jackson, *J. Am. Chem. Soc.* **2005**, *127*, 4986 – 4987.

[21] Y. Nicolas, P. Blanchard, J. Roncalli, M. Allain, N. Mercier, A.-L. Deman, J. Tardy, *Org. Lett.* **2005**, *7*, 3513 – 3516.

[22] a) D. Fichou, G. G. Horowitz, F. Garnier, Eur. Pat. App. EP 402,269, **1990**; b) V. M. Niemi, P. Knuuttila, J.-E. Österholm, J. Korvola, *Polymer* **1992**, *33*, 1559 – 1562; c) M. S. A. Abdou, X. Lu, Z. W. Xie, F. Orfino, M. J. Deen, S. Holdcroft, *Chem. Mater.* **1995**, *7*, 631 – 641; d) G. Engelmann, W. Jugelt, G. Kossmehl, H.-P. Welzel, P. Tschuncky, J. Heinze, *Macromolecules* **1996**, *29*, 3370 – 3375.

[23] a) T. Kauffmann, *Angew. Chem.* **1974**, *86*, 321 – 325; *Angew. Chem. Int. Ed. Engl.* **1974**, *13*, 291 – 305; b) J. Kagan, S. K. Arora, *Heterocycles* **1983**, *20*, 1937 – 1940; c) F. Garnier, A. Yassar, R. Hajlaoui, G. Horowitz, F. Deloffre, B. Servet, S. W. Ries, P. Alnot, *J. Am. Chem. Soc.* **1993**, *115*, 8716 – 8721; d) M. J. Marsella, T. M. Swager, *J. Am. Chem. Soc.* **1993**, *115*, 12214 – 12215.

[24] a) T. Yamamoto, K. Sanechita, A. Yamamoto, *Bull. Chem Soc. Jpn.* **1983**, *56*, 1497 – 1502;b) K. Tamao, K. Sumitani, M. Kumada, *J. Am. Chem. Soc.* **1972**, *94*, 4374 – 4376; c) M. Kumada, *Pure Appl. Chem.* **1980**, *52*, 669 – 679; d) K. Tamao, S. Kodama, I. Nakajima, M. Kumada, A. Minato, K. Suzuki, *Tetrahedron* **1982**, *38*, 3347 – 3354; e) P. Bäuerle, F. Würthner, G. Götz, F. Effenberger, *Synthesis* **1993**, 1099 – 1103.

[25] a) D. Milstein, J. K. Stille, *J. Am. Chem. Soc.* **1978**, *100*, 3636; b) J. K. Stille, *Angew. Chem.* **1986**, *98*, 504 – 519; *Angew. Chem. Int. Ed. Engl.* **1986**, *25*, 508 – 524; c) T. N. Mitchell, *Synthesis* **1992**, 803 – 815; d) V. Farina, *Pure Appl. Chem.* **1996**, *68*, 73 – 78; e) R. Hajlaoui, D. Fichou, G. Horowitz, B. Nessakh, M. Constant, F. Garnier, *Adv. Mater.* **1997**, *9*, 557 – 561.

[26] a) N. Miyaura, A. Suzuki, *Chem. Rev.* **1995**, *95*, 2457 – 2483; b) N. Miyaura, *Top. Curr. Chem.* **2002**, *219*, 11 – 59.

[27] F. Garnier, F. Deloffre, G. Horowitz, R. Hajlaoui, *Synth. Met.* **1993**, *57*, 4747 – 4754.

[28] a) F. Garnier, A. Yassar, R. Hajlaoui, G. Horowitz, F. Deloffre, B. Servet, Simone Ries, P. Alnot, *J. Am. Chem. Soc.* **1993**, *115*, 8716 – 8721; b) C. D. Dimitrakropoulos, B. K. Fuhrman, T. Graham, S. Hedge, S. Purushothaman, *Synth. Met.* **1998**, *92*, 47 – 52.

[29] a) M. Halik, H. Klauk, U. Zschieschang, G. Schmid, W. Radlik, S. Ponomarenko, S. Kirchmeyer, W. Weber, *J. Appl. Phys.* **2003**, *93*, 2977 – 2981; b) M. Halik, H. Klauk, U. Zschieschang, G. Schmid, W. Radlik, S. Ponomarenko, S. Kirchmeyer, W. Weber, *Adv. Mater.* **2003**, *15*, 917 – 922.

[30] a) F. Garnier, R. Hajlaoui, G. Horowitz, L. Laigre, W. Porzio, M. Armanini, F. Provasoli, *Chem. Mater.* **1998**, *10*, 3334 – 3339; b) S. Ponomarenko, S. Kirchmeyer, *J. Mater. Chem.* **2003**, *13*, 197 – 202.

[31] K. R. Amundson, H. E. Katz, A. J. Lovinger, *Thin Solid Films* **2003**, *426*, 140 – 149.

[32] H. E. Katz, A. J. Lovinger, J. Laquindanum, *Synth. Met.* **1999**, *102*, 897 – 899.

[33] S. A. Ponomarenko, S. Kirchmeyer, A. Elschner, B.-H. Huisman, A. Karbach, D. Drechsler, *Adv. Funct. Mater.* **2003**, *13*, 591 – 596.

[34] a) Y. Sun, K. Xiao, Y. Liu, J. Wang, J. Pei, G. Yu, D. Zhu, *Adv. Funct. Mater.* **2005**, *15*, 818 – 822; b) J. Pei, J.-L. Wang, X.-Y. Cao, X.-H. Zhou, W.-B. Zhang, *J. Am. Chem. Soc.* **2003**, *125*, 9944 – 9945; c) J. Pei, J. Ni, X.-H. Zhou, X.-Y. Cao, Y.-H. Lai, *J. Org. Chem.* **2002**, *67*, 4924 – 4936.

[35] S. A. Ponomarenko, E. A. Tatarinova, A. M. Muzafarov, S. Kirchmeyer, L. Brassat, A. Mourran, M. Moeller, S. Setayesh, D. de Leeuw, *Chem. Mater.* **2006**, *18*, 4101 – 4108.

[36] a) B. S. Nehls, F. Galbrecht, A. Bilge, U. Scherf, T. Farrell, *Macromol. Symp.* **2006**, *239*, 21 – 29; b) A. Zen, A. Bilge, F. Galbrecht, R. Alle, K. Meerholz, J. Grenzer, D. Neher, U. Scherf, T. Farrell, *J. Am. Chem. Soc.* **2006**, *128*, 3914 – 3915; c) A. Bilge, A. Zen, M. Forster, H. Li, F. Galbrecht, B. S. Nehls, T. Farrell, D. Neher, U. Scherf, *J. Mater. Chem.* **2006**, *16*, 3177 – 3182.

[37] R. Wu, J. S. Schumm, D. L. Pearson, J. M. Tour, *Org. Chem.* **1996**, *61*, 6906 – 6921.

[38] a) A. R. Murphy, J. M. J. Fréchet, P. Chang, J. Lee, V. Subramanian, *J. Am. Chem. Soc.* **2004**, *126*, 1596 – 1597; b) P. C. Chang, J. Lee, D. Huang, V. Subramanian, A. R. Murphy, J. M. J. Fréchet, *Chem. Mater.* **2004**, *16*, 4783 – 4789; c) A. R. Murphy, P. C. Chang, P. VanDyke, J. Liu, J. M. J. Fréchet, V. Subramanian, D. M. DeLongchamp, S. Sambasivan, D. A. Fischer, E. K. Lin, *Chem. Mater.* **2005**, *17*, 6033 – 6041; d) D. M. DeLongchamp, S. Sambasivan, D. A. Fischer, E. K. Lin, P. Chang, A. R. Murphy, J. M. J. Fréchet, V. Subramanian, *Adv. Mater.* **2005**, *17*, 2340 – 2344.

[39] H. Thiem, P. Strohriegl, S. Setayesh, D. de Leeuw, *Synth. Met.* **2006**, *156*, 582 – 589.
[40] a) H. Meng, Z. Bao, A. J. Lovinger, B. C. Wang, A. M. Mujsce, *J. Am. Chem. Soc.* **2001**, *123*, 9214 – 9215; b) H. Meng, J. Zheng, A. J. Lovinger, B. C. Wang, P. G. van Patten, Z. Bao, A. M. Mujsce, *Chem. Mater.* **2003**, *15*, 1778 – 1787.
[41] D. Adam, P. Schuhmacher, J. Simmerer, L. Haussling, K. Siemensmeyer, K. H. Etzbach, H. Ringsdorf, D. Haarer, *Nature* **1994**, *371*, 141 – 143.
[42] a) Ref. [30a]; b) Ref. [31].
[43] I. McCulloch, W. Zhang, C. Bailey, M. Giles, D. Graham, M. Shkunov, D. Sparrowe, S. Tierney, *J. Mater. Chem.* **2003**, *13*, 2436 – 2444.
[44] A. J. J. M. van Breemen, P. T. Herwig, C. H. T. chlon, J. Sweelssen, H. F. M. Schoo, S. Setayesh, W. M. Hardemann, C. A. Marin D. M. de Leeuw, J. J. P. Valeton, C. W. M. Bastiaansen, D. J. Broer, A. R. Popa-Merticaru, S. C. J. Meskers, *J. Am. Chem. Soc.* **2006**, *128*, 2336 – 2345.
[45] a) A. Stabel, P. Herwig, K. Müllen, J. P. Rabe, *Angew. Chem.* **1995**, *34*, 1768 – 1770; *Angew. Chem. Int. Ed. Engl.* **1995**, *34*, 1609 – 1611; b) P. Herwig, C. W. Kayser, K. Müllen, H. W. Spiess, *Adv. Mater.* **1996**, *8*, 510 – 513.
[46] M. G. Debije, J. Piris, M. P. de Haas, J. M. Warman, Z. Tomovic, C. D. Simpson, M. D. Watson, K. Müllen, *J. Am. Chem. Soc.* **2004**, *126*, 4641 – 4645.
[47] a) P. Miskiewicz, A. Ryback, J. Jung, I. Glowacki, J. Ulanski, Y. Geerts, M. Watson, K. Müllen, *Synth. Met.* **2003**, *137*, 905 – 906; b) W. Pisula, A. Menon, M. Stepputat, I. Lieberwirth, U. Kolb, A. Tracz, H. Sirringhaus, T. Pakula, K. Müllen, *Adv. Mater.* **2005**, *17*, 684 – 689.
[48] a) A. Grimsdale, K. Müllen, *Angew. Chem.* **2005**, *117*, 5732 – 5772; *Angew. Chem. Int. Ed.* 2005, 44, 5592 – 5629; b) W. Pisula, Z. Tomovic, M. Stepputat, U. Kolb, T. Pakula, K. Müllen, *Chem. Mater.* **2005**, *17*, 2641 – 2647; c) I. O. Shklyarevskiy, P. Jonkheijm, N. Stutzmann, D. Wasserberg, H. J. Wondergem, P. C. M. Christianen, A. P. H. J. Schenning, D. M. de Leeuw, Z. Tomovic, J. Wu, K. Müllen, J. C. Maan, *J. Am. Chem. Soc.* **2005**, *127*, 16233 – 16237.
[49] a) T. Yamamoto, K. Sanechika, A. Yamamoto, *J. Polym. Sci. Polym. Lett. Ed.* **1981**, *13*, 255 – 261; b) J. W. P. Lin, L. P. Dudeck, *J. Polym. Sci. Polym. Chem. Ed.* **1980**, *18*, 2869 – 2875.
[50] a) A. Tsumura, H. Koezuka, T. Ando, *Appl. Phys. Lett.* **1986**, *49*, 1210 – 1212; b) A. Tsumura, H. Koezuka, T. Ando, *Synth. Met.* **1988**, *25*, 11 – 23.
[51] K. Y. Jen, R. Oboodi, R. L. Elsenbaumer, *Polym. Mater. Sci. Eng.* **1985**, *53*, 79 – 83; R. L. Elsenbaumer, K. Y. Jen, R. Oboodi, *Synth. Met.* **1986**, *15*, 169 – 174; G. G. Miller, R. L. Elsenbaumer, *J. Chem. Soc. Chem. Commun.* **1986**, 873 – 875.
[52] a) R. J. Waldman, J. Bargon, A. F. Diaz, *J. Phys. Chem.* **1983**, *87*, 1459 – 1463; b) R. I. Sugimoto, S. Takeda, H. B. Gu, K. Yoshino, *Chem. Express* **1986**, *11*, 635 – 638; c) R. D. McCullough, R. D. Loewe, *J. Chem. Soc. Chem. Commun.* **1992**, *1*, 70 – 72; d) A. Iraqi, G. W. Barker, *J. Mater. Chem.* **1998**, *8*, 25 – 29; e) S. Gullierez, G. Bidan, *Synth. Met.* **1998**, *93*, 123 – 126; f) X. Wu, T.-A. Chen, R. D. Rieke, *Macromolecules* **1995**, *28*, 2101 – 2102; g) R. S. Loewe, R. D. McCullough, *Polymer preprints* **1999**, *40*, 852 – 853.
[53] a) A. Assadi, C. Svensson, M. Willander, O. Inganäs, *Appl. Phys. Lett.* **1988**, *53*, 195 – 197; b) A. Tsumura, H. Fuchigami, H. Koezuka, *Synth. Met.* **1991**, *41*, 1181 – 1184.
[54] a) T. A. Chen, X. Wu, R. D. Rieke, *J. Am. Chem. Soc.* **1995**, *117*, 233 – 244; b) R. S. Loewe, P. C. Ewbank, J. Liu, L. Zhai, R. D. McCullough, *Macromolecules* **2001**, *34*, 4324 – 4333.
[55] a) Z. Bao, A. Dodabalapur, A. J. Lovinger, *Appl. Phys. Lett.* **1996**, *69*, 4108 – 4110; b) H. Sirringhaus, P. J. Brown, R. H. Friend, M. M. Nielsen, K. Bechgaard, B. M. W. Langeveld-Voss, A. J. H. Spiering, R. A. J. Janssen, E. W. Meijer, P. T. Herwig, D. M. de Leeuw, *Nature* **1999**, *401*, 685 – 688.
[56] Ref. [54a].
[57] a) T. J. Prosa, M. J. Winokur, J. Moulton, P. Smith, A. J. Heeger, *Macromolecules* **1992**, *25*, 4364 – 4372; b) A. Tsumura, A. Fuchigami, H. Koezuka, *Synth. Met.* **1991**, *41*, 1181 – 1183; c) H. Sirringhaus, P. J. Brown, R. H. Friend, M. M. Nielsen, K. Bechgaard, B. J. Janssen, E. W. Meijer, P. T. Herwig, D. M. de Leeuw, *Nature* **1999**, *401*, 685 – 688.
[58] a) J. Paloheimo, H. Strubb, P. Yli-Lathi, P. Kuivalainen, *Synth. Met.* **1991**, *41*, 563 – 566; b) C. D. Dimitrakopoulos, D. J. Mascaro, *IBM J. Res. Dev.* **2001**, *45*, 11 – 27.
[59] A. Zen, J. Pflaum, S. Hirschmann, W. Zhuang, F. Jaiser, U. Asawapirom, R. P. Rabe, U. Scherf, D. Neher, *Adv. Funct. Mater.* **2004**, *14*, 757 – 764.
[60] a) R. J. Kline, M. D. McGehee, E. N. Kadnikova, J. Liu, J. M. J. Frechet, M. F. Toney, *Macromolecules* **2005**, *38*, 3312 – 3319; b) R. J. Kline, M. D. McGehee, E. N. Kadnikova, J. Liu, J. M. J. Frechet, *Adv. Mater.* **2003**, *15*, 1519 – 1522.
[61] J. Chang, B. Sun, D. W. Breiby, M. M. Nielsen, T. I. Solling, M. Giles, I. McCulloch, H. Sirringhaus, *Chem. Mater.* **2004**, *16*, 4772 – 4776.
[62] a) A. Zen, M. Saphiannikova, D. Neher, J. Grenzer, S. Grigorian, U. Pietsch, U. Asawapirom, U. Scherf, *Macromolecules* **2006**, *39*, 2162 – 2171; b) A. Zen, D. Neher, K. Silmy, A. Holländer, U. Asawapirom, U. Scherf, *Jpn. J. Appl. Phys. Part 1* **2005**, *44*, 3721 – 3727.
[63] a) J. Ficker, A. Ullmann, W. Fix, H. Rost, W. Clemens, *J. Appl. Phys.* **2003**, *94*, 2638 – 2641; b) J. Ficker, H. von Seggern, W. Fix, H. Rost, W. Clemens, I. McCulloch, *Appl. Phys. Lett.* **2004**, *85*, 1377 – 1379; c) M. S. A. Abdou, F. P. Orfino, Y. Son, S. Holdcroft, *J. Am. Chem. Soc.* **1997**, *119*, 4518 – 4524.
[64] a) H. Sirringhaus, *Adv. Mater.* **2005**, *17*, 2411 – 2425; b) B. S. Ong, Y. L. Wu, P. Liu, S. Gardener, *J. Am. Chem. Soc.* **2004**, *126*, 3378 – 3379; c) M. Heeney, C. Bailey, K. Genevicius, M. Shkunov, D. Sparrowe, S. Tierney, I. McCulloch, *J. Am. Chem. Soc.* **2005**, *127*, 1078 – 1079.
[65] a) B. S. Ong, Y. Wu, P. Liu, S. Gardner, *J. Am. Chem. Soc.* **2004**, *126*, 3378 – 3379; b) N. Zhao, G. A. Botton, S. Zhu, A. Duft, B. S. Ong, Y. Wu, P. Liu, *Macromolecules* **2004**, *37*, 8307 – 8312; c) B. S. Ong, Y. Wu, P. Liu, S. Gardener, *Adv. Mater.* **2005**, *17*, 1141 – 1144.
[66] Y. Wu, P. Liu, S. Gardner, B. S. Ong, *Chem. Mater.* **2005**, *17*, 221 – 223.
[67] a) B. S. Ong, Y. Wu, L. Jiang, P. Liu, K. Murti, *Synth. Met.* **2004**, *142*, 49 – 52; b) R. Pokrop, J.-M. Verilhac, A. Gasoir, I. Wielgus, M. Zagorska, J.-P. Travers, A. Prom, *J. Mater. Chem.* **2006**, *16*, 3099 – 3106.
[68] I. McCulloch, C. Bailey, M. Giles, M. Heeney, I. Love, M. Shkunov, D. Sparrow, S. Tierney, *Chem. Mater.* **2005**, *17*, 1381 – 1385.
[69] a) I. McCulloch, M. Heeney, C. Bailey, K. Genevicius, I. Macdonald, M. Shkunov, D. Sparrowe, S. Tierney, R. Wagner, W. Zhang, M. L. Chabinyc, R. J. Kline, M. D. McGehee, M. F. Toney, *Nat. Mater.* **2006**, *5*, 328 – 333; b) M. L. Chabinyc, M. F. Toney, R. J. Kline, I. McCulloch, M. Heeney, *J. Am. Chem. Soc.* **2007**, *129*, 3226 – 3237; c) D. M. DeLongchamp, R. J. Kline, E. K. Lin, D. A. Fischer, L. J. Richter, L. A. Lucas, M. Heeney, I. McCulloch, J. E. Northrup, *Adv. Mater.* **2007**, *19*, 833 – 837.
[70] H. Pan, Y. Li, Y. Wu, P. Liu, B. S. Ong, S. Zhu G. Xu, *J. Am. Chem. Soc.* **2007**, *129*, 4112 – 4113.
[71] a) M. Bernius, M. Inbasekaran, E. Woo, W. Wu, L. Wujukowski, *J. Mater. Sci. Mater. Electron.* **2000**, *11*, 111 – 116; b) M. Redecker, D. D. C. Bradley, M. Inbasekaran, E. P. Woo, *Appl. Phys. Lett.* **1999**, *74*, 1400 – 1402; c) M. Grell, M. Redecker, K. S. Whitehead, D. D. C. Bradley, M. Inbasekaran, E. P. Woo, W. Wu,

Liq. Cryst. **1999**, *26*, 1403 – 1407; d) D. Hertel, U. Scherf, H. Bässler, *Adv. Mater.* **1998**, *10*, 1119 – 1122.
[72] A. Babel, S. A. Jenekhe, *Macromolecules* **2003**, *36*, 7759 – 7764.
[73] a) T. Yasuda, K. Fujita, T. Tsutsui, Y. Geng, S. W. Culligan, S. H. Chen, *Chem. Mater.* **2005**, *17*, 264 – 268; b) A. Bolognesi, A. Dicarlo, P. Lugli, *Appl. Phys. Lett.* 2002, 81, 4646 – 4648; c) M. Grell, D. D. C. Bradley, X. Long, M. Inbasekaran, E. P. Woo, M. Soliman, *Acta Polym.* **1998**, *49*, 439 – 444.
[74] M. Heeney, C. Bailey, M. Giles, M. Shkunov, D. Sparrowe, S. Tierney, W. Zhang, I. McColloch, *Macromolecules* **2004**, *37*, 5250 – 5256.
[75] a) M. Heeney, C. Bailey, M. Giles, M. Shkunov, D. Sparrowe, S. Tierney, W. Zhang, I. McColloch, *Macromolecules* **2004**, *37*, 5250 – 5256; b) T. Yamamoto, D. Komarudin, M. Arai, B.-L. Lee, H. Suganuma, N. Asakawa, Y. Inoue, K. Kubota, S. Sasaki, T. Fukuda, H. Matsuda, *J. Am. Chem. Soc.* **1998**, *120*, 2047 – 2058.
[76] a) M. Inbasekaran, W. Wu, E. P. Woo, US Patent, WO 5.777.070, **1998**; b) M. Grell, D. D. C. Bradley, X. Long, M. Inbasekaran, E. P. Woo, M. Soliman, *Acta Polym.* **1998**, *49*, 439 – 444; c) L. Kinder, J. Kanicki, P. Petroff, *Synth. Met.* **2004**, *146*, 181 – 185.
[77] a) H. Sirringhaus, R. J. Wilson, R. H. Friend, M. Inbasekaran, W. Wu, E. P. Woo, M. Grell, D. C. C. Bradley, *Appl. Phys. Lett.* **2000**, *77*, 406 – 408; b) H. Sirringhaus, N. Tessler, D. S. Thomas, P. J. Brown, R. H. Friend in *Advances in Solid State Physics*, *vol. 39* (Ed.: B. Kramer), Vieweg, Braunschweig, **1999**, S. 101; c) D. J. Brennan, P. H. Townend, D. M. Welsh, M. G. Dibbs, J. M. Shaw, J. L. Miklovich, R. B. Boeke, *Mater. Res. Soc. Symp. Proc.* **2003**, *771*, L6.1.1 – L6.1.6; d) H. Sirringhaus, T. Kawase, R. H. Friend, T. Shimoda, M. Inbasekaran, W. Wu, E. P. Woo, *Science* **2000**, *290*, 2123 – 2126.
[78] H. Sirringhaus, T. Kawase, R. H. Friend, *MRS Bull.* **2001**, 539 – 543.
[79] S. P. Li, C. J. Newsome, D. M. Russell, T. Kugler, M. Ishida, T. Shimoda, *Appl. Phys. Lett.* **2005**, 06210.
[80] a) E. Lim, B.-J. Jung, J. Lee, H.-K. Shim, J.-I. Lee, Y. S. Yang, L.-M. Do, *Macromolecules* **2005**, *38*, 4531 – 4535; b) C. D. Dimitrakopoulous, S. Purushothaman, J. Kymissis, A. Callegari, M. J. Shaw, *Science* **1998**, *283*, 822 – 824; c) J. G. Laquindanum, H. E. Katz, A. J. Lovinger, *J. Am. Chem. Soc.* **1998**, *120*, 664 – 667.
[81] a) U. Asawapirom, R. Güntner, M. Forster, T. Farrell, U. Scherf, *Synthesis* **2002**, 1136 – 1142; b) B. S. Nehls, U. Asawapirom, S. Füldner, E. Preis, T. Farrell, U. Scherf, *Adv. Func. Mater.* **2004**, *14*, 352 – 356; c) U. Asawapirom, *Flüssigkristalline Polymere und Copolymere auf Thiophenbasis*, Dissertation, Bergische Universität-Gesamthochschule Wuppertal, **2003**.
[82] a) M. Zhang, H. N. Tsao, W. Pisula, A. K. Mishra, K. Müllen, *J. Am. Chem. Soc.* **2007**, *129*, 3472 – 3473; b) D. Mühlbacher, M. Scharber, M. Morana, Z. Zhu, D. Waller, R. Gaudiana, C. Brabec, *Adv. Mater.* **2006**, *18*, 2884 – 2889.
[83] a) S. Yamada, S. Tokito, T. Tsutsui, S. Saito, *J. Chem. Soc. Chem. Commun.* **1987**, 1448 – 1449; b) I. Murase, T. Ohnishi, T. Noguchi, M. Hirooka, *Polym. Commun.* **1987**, 28, 229 – 230.
[84] H. Fuchigami, A. Tsumura, H. Koezuka, *Appl. Phys. Lett.* **1993**, *63*, 1372 – 1374.
[85] C. J. Drury, C. M. J. Mutsaers, C. M. Hart, M. Matters, D. M. De Leeuw, *Appl. Phys. Lett.* **1998**, *73*, 108 – 110.
[86] a) H. G. Gilch, W. L. Wheelwright, *J. Polym. Sci.* **1966**, *4*, 1137 – 1349; b) R. A. Wessling, R. G. Zimmerman, U.S. Patent No 3401152, **1968**; c) R. A. Wessling, *J. Polym. Sci. Part C* **1985**, *72*, 55 – 66; d) S. Son, A. Dodabalapur, A. J. Lovinger, M. E. Galvin, *Science* **1995**, *269*, 376 – 378; e) F. Louwet, D. Vanderzande, J. Gelan, *Synth. Met.* **1992**, *52*, 125 – 130; f) F. Louwet, D. Vanderzande, J. Gelan, *Synth. Met.* **1995**, *69*, 509 – 510; g) F. Louwet, D. Vanderzande, J. Gelan, J. Mullens, *Macromolecules* **1995**, *28*, 1330 – 1331.
[87] a) A. Henckens, L. Lutsen, D. Vanderzande, M. Knipper, J. Manca, T. Aernouts, J. Poortsmans, *Proc. SPIE-Int. Soc. Opt. Eng.* **2004**, *5464*, 52 – 59; b) S. Gillissen, A. Henckens, L. Lutsen, D. Vanderzande, J. Gelan, *Synth. Met.* **2003**, *135–136*, 255 – 256.
[88] P. Prins, L. P. Candeias, A. J. J. M. van Breemen, J. Sweelssen, P. T. Herwig, H. F. M. Schoo, L. D. A. Siebbels, *Adv. Mater.* **2005**, *17*, 718 – 723.
[89] a) R. Kisselev, M. Thelakkat, *Macromolecules* **2004**, *37*, 8951 – 8958; b) J. Ostraukaite, M. Thelakkat, M. Heim, R. Bilke, D. Haarer, *Synth. Met.* **2001**, *121*, 1573 – 1574; c) C. Jäger, R. Bilke, M. Heim, D. Haarer, K. R. Haridas, M. Thelakkat, *Synth. Met.* **2001**, *121*, 1543 – 1544; d) M. Thelakkat, J. Hagen, D. Haarer, H. W. Schmidt, *Synth. Met.* **1999**, *102*, 1125 – 1128; e) M. Thelakkat, *Macromol. Mater. Eng.* **2002**, *287*, 442 – 461; f) Y. Shirota, *J. Mater. Chem.* **2005**, *15*, 75 – 93; g) P. M. Borsenberger, L. Pautmeier, H. Bässler, *J. Chem. Phys.* **1991**, *94*, 5447 – 5454.
[90] a) E. T. Seo, R. F. Nelson, J. M. Fritsch, L. S. Marcoux, D. W. Leedy, R. N. Adams, *J. Am. Chem. Soc.* **1966**, *88*, 3498 – 3503; b) R. F. Nelson, R. N. Adams, *J. Am. Chem. Soc.* **1968**, *90*, 3925 – 3930.
[91] a) C. Kvarnström, A. Petr, P. Damlin, T. Lindfors, A. Ivaska, L. Dunsch, *J. Solid State Electrochem.* **2002**, *6*, 505 – 512; b) A. Petr, C. Kvarnström, L. Dunsch, A. Ivaska, *Synth. Met.* **2000**, *108*, 245 – 247; c) C. Lambert, G. Nöll, *Synth. Met.* **2003**, *139*, 57 – 62.
[92] a) J. Louie, J. F. Hartwig, *Tetrahedron Lett.* **1995**, *36*, 3609 – 3612; b) J. F. Hartwig, *Synlett* **1997**, 329 – 340; c) J. F. Hartwig, *Angew. Chem.* **1998**, *110*, 2154 – 2177; *Angew. Chem. Int. Ed.* **1998**, *37*, 2046 – 2067; d) A. S. Guram, R. A. Rennels, S. L. Buchwald, *Angew. Chem.* **1995**, *107*, 1456 – 1459; *Angew. Chem. Int. Ed. Engl.* **1995**, *34*, 1348 – 1350; e) J. P. Wolfe, S. L. Buchwald, *J. Org. Chem.* **1996**, *61*, 1133 – 1135; f) B. H. Yang, S. L. Buchwald, *J. Organomet. Chem.* **1999**, *576*, 125 – 146.
[93] F. E. Goodson, S. I. Hauck, J. F. Hartwig, *J. Am. Chem. Soc.* **1999**, *121*, 7527 – 7539.
[94] J. Veres, S. D. Ogier, S. W. Leeming, B. Brown, D. C. Cupertino, *Mater. Res. Soc. Symp. Proc.* **2002**, *708*, BB8.7.1 – BB8.7.8.
[95] a) L. A. Majewski, M. Grell, S. D. Ogier, J. Veres, *Org. Electron.* **2003**, *4*, 27 – 32; b) J. Veres, S. D. Ogier, S. W. Leeming, D. C. Cupertino, S. M. Khaffaf, *Adv. Funct. Mater.* **2003**, *13*, 199 – 204; c) J. Veres, S. D. Ogier, G. Lloyd, D. de Leeuw, *Chem. Mater.* **2004**, *16*, 4543 – 4555.
[96] a) Ref. [9d]; b) D. Zielke, A. C. Hübler, U. Hahn, N. Brandt, M. Bartzsch, U. Fügmann, T. Fischer, J. Veres, S. D. Ogier, *Appl. Phys. Lett.* **2005**, *87*, 123508.
[97] a) Y. Wu, Y. Li, S. Gardner, B. S. Ong, *J. Am. Chem. Soc.* **2005**, *127*, 614 – 618; b) Y. Wu, Y. Li, S. Gardner, B. S. Ong, *Adv. Mater.* **2005**, *17*, 849 – 853; c) Y. Wu, Y. Li, S. Gardner, B. S. Ong, *Macromolecules* **2006**, *39*, 6521 – 6527.

